

1 **Phage infection and sub-lethal antibiotic exposure mediate *Enterococcus faecalis* type**

2 **VII secretion system dependent inhibition of bystander bacteria**

3

4 Anushila Chatterjee^{a*}, Julia L. E. Willett^{b*}, Gary M. Dunny^b, Breck A. Duerkop^{a,#}

5

6 ^aDepartment of Immunology and Microbiology, University of Colorado School of Medicine,

7 Aurora, CO, USA, 80045. ^bDepartment of Microbiology and Immunology, University of

8 Minnesota Medical School, Minneapolis, MN, USA, 55455.

9

10 #Correspondence: Breck A. Duerkop breck.duerkop@cuanschutz.edu

11 *A.C. and J.L.E.W. contributed equally to this work.

12

13

14 Running title: Phage and antibiotic induced T7SS promotes antibacterial antagonism

15

16 Key words: bacteriophages, *Enterococcus*, antibiotic resistance, phage–bacteria interactions,

17 bacterial secretion systems, type VII secretion, contact-dependent antagonism

18

19

20

21

22

23

24

25

26

27 **Abstract**

28 Bacteriophages (phages) are being considered as alternative therapeutics for the treatment
29 of multidrug resistant bacterial infections. Considering phages have narrow host-ranges, it is
30 generally accepted that therapeutic phages will have a marginal impact on non-target bacteria.
31 We have discovered that lytic phage infection induces transcription of type VIIIb secretion
32 system (T7SS) genes in the pathobiont *Enterococcus faecalis*. Membrane damage during
33 phage infection induces T7SS gene expression resulting in cell contact dependent antagonism
34 of different Gram positive bystander bacteria. Deletion of *essB*, a T7SS structural component,
35 abrogates phage-mediated killing of bystanders. A predicted immunity gene confers protection
36 against T7SS mediated inhibition, and disruption of its upstream LXG toxin gene rescues growth
37 of *E. faecalis* and *Staphylococcus aureus* bystanders. Phage induction of T7SS gene
38 expression and bystander inhibition requires IreK, a serine/threonine kinase, and
39 OG1RF_11099, a predicted GntR-family transcription factor. Additionally, sub-lethal doses of
40 membrane targeting and DNA damaging antibiotics activated T7SS expression independent of
41 phage infection, triggering T7SS antibacterial activity against bystander bacteria. Our findings
42 highlight how phage infection and antibiotic exposure of a target bacterium can affect non-target
43 bystander bacteria and implies that therapies beyond antibiotics, such as phage therapy, could
44 impose collateral damage to polymicrobial communities.

45

46 **Author Summary**

47 Renewed interest in phages as alternative therapeutics to combat multi-drug resistant
48 bacterial infections, highlights the importance of understanding the consequences of phage-
49 bacteria interactions in the context of microbial communities. Although it is well established that
50 phages are highly specific for their host bacterium, there is no clear consensus on whether or
51 not phage infection (and thus phage therapy) would impose collateral damage to non-target
52 bacteria in polymicrobial communities. Here we provide direct evidence of how phage infection

53 of a clinically relevant pathogen triggers an intrinsic type VII secretion system (T7SS)
54 antibacterial response that consequently restricts the growth of neighboring bacterial cells that
55 are not susceptible to phage infection. Phage induction of T7SS activity is a stress response
56 and in addition to phages, T7SS antagonism can be induced using sub-inhibitory concentrations
57 of antibiotics that facilitate membrane or DNA damage. Together these data show that a
58 bacterial pathogen responds to diverse stressors to induce T7SS activity which manifests
59 through the antagonism of neighboring non-kin bystander bacterial cells.

60

61 **Introduction**

62 Enterococci constitute a minor component of the healthy human microbiota [1]. Enterococci,
63 including *Enterococcus faecalis*, are also nosocomial pathogens that cause a variety of
64 diseases, including sepsis, endocarditis, surgical-site, urinary tract and mixed bacterial
65 infections [2, 3]. Over recent decades, enterococci have acquired extensive antibiotic resistance
66 traits, including resistance to “last-resort” antibiotics such as vancomycin, daptomycin, and
67 linezolid [4-8]. Following antibiotic therapy, multi-drug resistant (MDR) enterococci can outgrow
68 to become a dominant member of the intestinal microbiota, resulting in intestinal barrier invasion
69 and blood stream infection [7, 9]. The ongoing evolution of MDR enterococci in healthcare
70 settings [4-6, 10, 11] and their ability to transmit antibiotic resistance among diverse bacteria [9,
71 12-15], emphasize the immediate need for novel therapeutic approaches to control enterococcal
72 infections.

73 Viruses that infect and kill bacteria (bacteriophages or phages) are receiving attention for
74 their use as antibacterial agents [16]. Recent studies have demonstrated the efficacy of anti-
75 enterococcal phages in murine models of bacteremia [17-19] and the administration of phages
76 to reduce *E. faecalis* burden in the intestine gives rise to phage resistant isolates that are
77 sensitized to antibiotics [20]. Considering phages are highly specific for their target bacterium,
78 coupled with the self-limiting nature of their host-dependent replication, this suggests that unlike

79 antibiotics which have broad off-target antimicrobial activity, phages should have nominal
80 impact on bacteria outside of their intended target strain [21-23]. However, our understanding of
81 how phages interact with bacteria and the bacterial response to phage infection is limited.

82 While studying the transcriptional response of phage infected *E. faecalis* cells, we
83 discovered that phage infection induces the expression of genes involved in the biosynthesis of
84 a type VIIb secretion system (T7SS) [24]. Firmicutes, including the enterococci, harbor diverse
85 T7SS genes encoding transmembrane and cytoplasmic proteins involved in the secretion of
86 protein substrates [25], and T7SSs promote antagonism of non-kin bacterial cells through
87 production of antibacterial effectors and/or toxins [26, 27]. The antibacterial activity of T7SSs
88 from staphylococci and streptococci are well characterized [25] but T7SS-mediated antibacterial
89 antagonism has not been described for enterococci. The environmental cues and regulatory
90 pathways that govern T7SS expression and activity are poorly understood, although recent
91 studies indicate that exposure to serum and membrane stresses triggered by pulmonary
92 surfactants, fatty acids and phage infection stimulate T7SS gene expression [24, 28-31]. This
93 motivated us to determine if phage induced T7SS gene expression in *E. faecalis* results in the
94 inhibition of non-kin bacterial cells that are not phage targets (bystanders). We discovered that
95 phage infected *E. faecalis* produces potent T7SS antibacterial activity against bystander
96 bacteria. Expression of a T7SS antitoxin (immunity factor) gene in bystander cells and mutation
97 of the LXG domain containing gene located immediately upstream of this immunity factor confer
98 protection against phage mediated T7SS inhibition. We also investigated the potential impact of
99 antimicrobials directed against bacterial physiological processes that are also targeted by
100 phages, including cell wall, cell membrane and DNA damaging agents, on enterococcal T7SS.
101 Sub-lethal challenge with specific antibiotics enhances T7SS gene expression resulting in T7SS
102 dependent interspecies antagonism. Additionally, we discovered that membrane stress during
103 phage infection induces transcription of T7SS genes via a non-canonical IreK signaling
104 pathway. To our knowledge, the enterococcal T7SS is the first example of secretion system

105 induction during phage infection. These data shed light on how phage infection of a cognate
106 bacterial host can influence polymicrobial interactions and raises the possibility that phages may
107 impose unintended compositional shifts among bystander bacteria in the microbiota during
108 phage therapy.

109

110 **Results**

111 **Phage mediated induction of *E. faecalis* T7SS leads to interspecies antagonism.**

112 A hallmark feature of phage therapy is that phages often have a narrow host range, hence
113 they do not influence the growth of non-susceptible bacteria occupying the same niche [22]. We
114 discovered that infection of *E. faecalis* OG1RF by phage VPE25 induces the expression of
115 T7SS genes [24]. The *E. faecalis* OG1RF T7SS locus is absent in the commonly studied
116 vancomycin-resistant strain V583, despite conservation of flanking genes (Fig. 1A) [32, 33]. The
117 OG1RF T7SS is found downstream of conserved tRNA-Tyr and tRNA-Gln genes, which could
118 facilitate recombination or integration of new DNA [34], but no known recombination or
119 integration sites were identified on the 3' end of this locus. Homologs of the *E. faecalis* T7SS
120 gene *esxA* are found throughout three of the four *Enterococcus* species groups [35], including
121 *Enterococcus faecium*, suggesting a wide distribution of T7SS loci in enterococci (Fig. S1). In
122 addition to *EsxA*, OG1RF encodes the core T7SS structural components *EsaA*, *EssB*, and
123 *EssC*, which are predicted to localize to the membrane, and *EsaB*, a small predicted
124 cytoplasmic protein (Fig. 1A) [36]. OG1RF_11102 encodes an additional putative membrane
125 protein, although it does not share sequence homology with staphylococcal or streptococcal
126 *EssA*. We were unable to identify an *EssA* homolog in OG1RF using sequence-based
127 homology searches, suggesting that the enterococcal T7SS machinery may differ from
128 previously described T7SS found in other Gram-positive bacteria. *In silico* analyses predict that
129 the *E. faecalis* T7SS locus encodes multiple WXG100 family effectors and LXG family
130 polymorphic toxins [27, 37]. We hypothesized that induction of T7SS genes during phage

131 infection and consequently the heightened production of T7SS substrates would indirectly
132 influence the growth of non-kin phage-resistant bacterial cells.

133 To investigate if T7SS factors produced during phage infection of *E. faecalis* OG1RF
134 interferes with the growth of phage-resistant bystander bacteria, we generated a strain with an
135 in-frame deletion in the T7SS gene *essB*, encoding a transmembrane protein involved in the
136 transport of T7SS substrates [38]. We chose to inactivate *essB* as opposed to the more
137 commonly investigated secretion promoting ATPase *essC* [27, 38], because *E. faecalis* OG1RF
138 harbours two *essC* genes in its T7SS locus that may have functional redundancy (Fig. 1A). The
139 *essB* mutant is equally susceptible to phage VPE25 infection compared to wild type *E. faecalis*
140 OG1RF (Fig. S2A). We performed co-culture experiments where phage susceptible wild type *E.*
141 *faecalis* OG1RF or Δ *essB* were mixed with a phage resistant bystander, a strain of *E. faecalis*
142 V583 deficient in the production of the VPE25 receptor (Δ *pip*_{V583}) [39], at a ratio of 1:1 in the
143 absence and presence of phage VPE25 (multiplicity of infection [MOI] = 0.01) (Fig. 1B). VPE25
144 infected *E. faecalis* OG1RF and the Δ *essB* mutant with similar efficiency and caused a 1000-
145 fold reduction in the viable cell count over a period of 24 hours relative to the starting cell count
146 (Fig. S2B). Since sequence-based homology searches did not retrieve any homologs of
147 potential antitoxins from the *E. faecalis* OG1RF T7SS locus in *E. faecalis* V583 genome, this
148 strain likely lacks immunity to toxins encoded in this locus. The viability of *E. faecalis* Δ *pip*_{V583},
149 was reduced nearly 100-fold when co-cultured with *E. faecalis* OG1RF in the presence of phage
150 VPE25 (Fig. 1C, S2C). However, growth inhibition of *E. faecalis* Δ *pip*_{V583} was abrogated during
151 co-culture with phage infected *E. faecalis* Δ *essB* and phage induced T7SS antagonism of *E.*
152 *faecalis* Δ *essB* could be restored by complementation (Fig. 1C, S2C), indicating that inhibition of
153 phage resistant *E. faecalis* Δ *pip*_{V583} by OG1RF is T7SS dependent.

154 T7SS encoded antibacterial toxins secreted by Gram positive bacteria influence intra- and
155 interspecies antagonism [26, 27]. While a nuclease and a membrane depolarizing toxin
156 produced by *Staphylococcus aureus* target closely related *S. aureus* strains [26, 40],

157 *Streptococcus intermedius* exhibits T7SS dependent antagonism against a wide-array of Gram
158 positive bacteria [27]. To determine the target range of *E. faecalis* OG1RF T7SS antibacterial
159 activity, we measured the viability of a panel of VPE25 insensitive Gram positive and Gram
160 negative bacteria in our co-culture assay (Fig. 1B). Growth inhibition of the distantly related
161 bacterial species *E. faecium* and Gram positive bacteria of diverse genera, including *S. aureus*
162 and *Listeria monocytogenes*, occurred following co-culture with phage infected wild type *E.*
163 *faecalis* OG1RF but not the Δ essB mutant (Fig. 1D). Fitness of *Lactococcus lactis*, a lactic acid
164 bacterium like *E. faecalis*, was modestly reduced during co-culture with phage infected *E.*
165 *faecalis* OG1RF, although these data were not statistically significant. In contrast, Gram positive
166 pathogenic and commensal streptococci were unaffected (Fig. 1D). Similarly, phage induced
167 T7SS activity did not inhibit any Gram negative bacteria tested (Fig. 1D). Collectively, these
168 results show that phage predation of *E. faecalis* promotes T7SS inhibition of select bystander
169 bacteria.

170

171 **Molecular basis of *E. faecalis* phage-triggered T7SS antagonism**

172 Our data demonstrate that induction of *E. faecalis* OG1RF T7SS genes during phage
173 infection hinder the growth of select non-kin bacterial species. Antibacterial toxins deployed by
174 Gram negative bacteria via type V and VI secretion and Gram positive T7SS require physical
175 contact between cells to achieve antagonism [26, 27, 41, 42]. Therefore, we investigated if
176 growth inhibition of bystander bacteria is contingent upon direct interaction with phage infected
177 *E. faecalis* using a trans-well assay [27]. We added unfiltered supernatants from wild type *E.*
178 *faecalis* OG1RF and Δ essB mutant cultures grown for 24 hrs in the presence and absence of
179 phage VPE25 (MOI = 0.01) to the top of a trans well and deposited phage resistant *E. faecalis*
180 Δ pip_{V583} in the bottom of the trans well. The 0.4 μ m membrane filter that separates the two wells
181 is permeable to proteins and solutes but prevents bacterial translocation. Supernatant from
182 phage infected wild type *E. faecalis* OG1RF did not inhibit *E. faecalis* Δ pip_{V583} (Fig. S3A)

183 indicating that T7SS mediated growth interference relies on cell to cell contact. To exclude the
184 possibility that T7SS substrates might adhere to the 0.4 μm membrane filter in the trans-well
185 assay, we administered both filtered and unfiltered culture supernatants directly to *E. faecalis*
186 Δpip_{V583} cells (5×10^5 CFU/well) at a ratio of 1:10 (supernatant to bystander cells) and monitored
187 growth over a period of 10 hours. Growth kinetics of *E. faecalis* Δpip_{V583} remained similar
188 irrespective of the presence or absence of conditioned supernatant from wild type *E. faecalis*
189 OG1RF or ΔessB mutant cultures (Fig. S3B – S3C), further supporting the requirement of
190 contact-dependent engagement of phage mediated T7SS inhibition.

191 We discovered that *E. faecalis* OG1RF inhibits proliferation of non-kin bacterial cells through
192 increased expression of T7SS genes in response to phage infection, but the toxic effectors were
193 unknown. LXG domain containing toxins are widespread in bacteria with a diverse range of
194 predicted antibacterial activities [43, 44]. The OG1RF T7SS locus encodes two LXG-domain
195 proteins, OG1RF_11109 and OG1RF_11121 (Fig. 2A). Both LXG domains were found using
196 Pfam, but we were unable to identify predicted function or activity for either protein using
197 sequence homology searches or structural modeling.

198 Bacterial polymorphic toxin systems can encode additional toxin fragments and cognate
199 immunity genes, known as “orphan” toxin/immunity modules, downstream of full-length secreted
200 effectors [45, 46]. Orphan toxins lack the N-terminal domains required for secretion or delivery,
201 although they can encode small regions of homology that could facilitate recombination with full-
202 length toxin genes [47]. Therefore, we sought to identify putative orphan toxins in OG1RF. We
203 aligned the nucleotide sequences of OG1RF_11109 and OG1RF_11121 with downstream
204 genes in the T7SS locus and looked for regions of similarity that might signify orphan toxins.
205 Although the 3' ends of OG1RF_11111 and OG1RF_11113 did not have homology to either
206 OG1RF_11109 or OG1RF_11121, the 5' ends of OG1RF_11111 and OG1RF_11113 had >75%
207 nucleotide homology to a portion of OG1RF_11109 (Fig. 2A, regions of homology indicated by
208 gray shading). Similarly, OG1RF_11123 had sequence homology to OG1RF_11121 (Fig. 2A).

209 We searched Pfam and ExPasy for annotated domains but were unable to identify any in
210 OG1RF_11111, OG1RF_11113, or OG1RF_11123. However, structural modeling with Phyre2
211 [48] revealed that a portion of OG1RF_11123 has predicted structural homology to the channel-
212 forming domain of colicin 1a [49] (Fig. S4D).

213 Orphan toxins encoded by a secretion system in a given strain can often be found as full-
214 length toxins in other bacteria [45, 46]. Therefore, we used the sequences of OG1RF_11111,
215 OG1RF_11113, and OG1RF_11123 as input for NCBI Protein BLAST to determine whether the
216 orphan toxins we identified in *E. faecalis* OG1RF were found in other T7SS loci. We identified
217 homologs to these orphan toxins in other *E. faecalis* strains as well as *Listeria* sp. (Fig. S4A-C,
218 gray shading indicates regions of homology). These homologs were longer than the *E. faecalis*
219 OG1RF genes and encoded N-terminal LXG domains, suggesting that in *Listeria* and other *E.*
220 *faecalis* strains, homologs to OG1RF_11111, 11113, and 11123 are full-length toxins that could
221 be secreted by the T7SS.

222 Interestingly, we identified an additional LXG gene product, OG1RF_12414, in a distal locus
223 that is again notably absent from *E. faecalis* V583 (Fig. S5A and S5B). OG1RF_12414 has
224 predicted structural homology to Tne2, a T6SS effector with NADase activity from
225 *Pseudomonas protegens* (Fig. S5C) [50]. Additionally, we identified numerous C-terminal
226 domains in LXG proteins distributed throughout the enterococci (Fig. S6). These include EndoU
227 and Ntox44 nuclease domains [43, 51, 52], which have been characterized in effectors
228 produced by other polymorphic toxin systems.

229 Polymorphic toxins are genetically linked to cognate immunity proteins that neutralize
230 antagonistic activity and prevent self-intoxication [43, 52, 53]. Each of the five putative toxins in
231 the OG1RF T7SS locus is encoded directly upstream of a small protein that could function in
232 immunity. Whitney *et al.* demonstrated that the cytoplasmic antagonistic activity of *S.*
233 *intermedius* LXG toxins TelA and TelB in *Escherichia coli* can be rescued by co-expression of
234 cognate immunity factors [27]. Therefore, we examined if OG1RF_11110, 11112, 11122, or

235 12413 confer immunity to *E. faecalis* Δpip_{V583} during phage infection of *E. faecalis* OG1RF.
236 Constitutive expression of OG1RF_11122, and not OG1RF_11110, 11112, or 12413, partially
237 neutralized phage induced T7SS antagonism (Fig. 2B), confirming an essential role for the
238 OG1RF_11122 gene product in immunity, and suggesting that OG1RF_11121 is at least partly
239 responsible for T7SS mediated intra-species antagonism. However, further investigation is
240 needed to confirm whether the candidate immunity factors, OG1RF_11110, 11112 or 12413,
241 are stably expressed under these experimental conditions.

242 To determine the contribution of OG1RF_11121 on intra- and interbacterial antagonism
243 during phage infection, we measured the viability of phage resistant *E. faecalis* Δpip_{V583} and *S.*
244 *aureus* in co-culture with an *E. faecalis* OG1RF variant carrying a transposon insertion in
245 OG1RF_11121 (OG1RF_11121-Tn). OG1RF_11121-Tn is equally susceptible to phage VPE25
246 infection compared to wild type *E. faecalis* OG1RF (Fig. S2A). Similar to the $\Delta essB$ (pCIEtm)
247 strain carrying empty pCIEtm plasmid, phage infected OG1RF_11121-Tn (pCIEtm) did not
248 inhibit the growth of the bystander bacteria (Fig. 2C – 2D). We were unable to clone
249 OG1RF_11121 by itself into the inducible plasmid pCIEtm, suggesting leaky expression of
250 OG1RF_11121 is toxic. Therefore, to complement *E. faecalis* OG1RF_11121-Tn we cloned
251 both the OG1RF_11121 toxin and OG1RF_11122 antitoxin pair under the cCF10-inducible
252 promoter in pCIEtm. Expression of both of these genes in the transposon mutant restored its
253 ability antagonize T7SS susceptible bystanders (Fig. 2C – D). These data strongly suggest that
254 the OG1RF_11121 encoded LXG toxin drives *E. faecalis* T7SS mediated antagonism of
255 bystanders following phage infection.

256

257 **Sub-lethal antibiotic stress promotes T7SS dependent antagonism**

258 Considering two genetically distinct phages trigger the induction of T7SS genes in *E.*
259 *faecalis* [24], we reasoned that T7SS induction could be a result of phage mediated cellular
260 damage and not specifically directed by a phage encoded protein. Antibiotics elicit a range of

261 damage induced stress responses in bacteria [54-56]; therefore, independent of phage infection
262 we investigated the effects of subinhibitory concentrations of antibiotics on T7SS expression in
263 *E. faecalis*.

264 To investigate the influence of sublethal antibiotic concentrations on *E. faecalis* OG1RF
265 T7SS transcription, we determined the minimum inhibitory concentrations (MIC) of ampicillin,
266 vancomycin, and daptomycin (Fig.S7A – S7C) and monitored T7SS gene expression in *E.*
267 *faecalis* OG1RF cells treated with a sub-lethal dose of antibiotic (50% of the MIC). We found
268 that bacterial T7SS genes were significantly upregulated in the presence of the cell membrane
269 targeting antibiotic, daptomycin, relative to the untreated control (Fig. 3A). In contrast, the cell
270 wall biosynthesis inhibitors ampicillin and vancomycin either did not induce or had a minor
271 impact on T7SS mRNA levels, respectively (Fig.3A). Additionally, induction of T7SS
272 transcription occurred when bacteria were challenged with sub-inhibitory concentrations of the
273 DNA targeting antibiotics ciprofloxacin and mitomycin C (Fig. 3B, Fig. S7D – S7E).

274 We next sought to assess the influence of daptomycin driven T7SS induction on inter-
275 enterococcal antagonism. *E. faecalis* V583 and its derivatives are more sensitive to daptomycin
276 compared to *E. faecalis* OG1RF strains (Fig. S8A – S8C), so we applied a reduced
277 concentration of 2.5 µg/ml daptomycin in the co-culture inhibition assay to prevent daptomycin
278 intoxication of *E. faecalis* Δpip_{V583} bystanders. Because *E. faecalis* OG1RF T7SS gene
279 expression is less robust in the presence of 2.5 µg/ml compared to 6.25 µg/ml daptomycin,
280 which was used in our previous experiments (Fig. 3A and S8D), a 10:1 ratio of daptomycin
281 treated *E. faecalis* OG1RF was required for growth inhibition of *E. faecalis* Δpip_{V583} during co-
282 culture (Fig. 3C). Consistent with our previous results, daptomycin induced T7SS inhibition of *E.*
283 *faecalis* Δpip_{V583} was contact dependent (Fig. 3D). To increase T7SS mediated contact-
284 dependent killing of the target strain during daptomycin exposure, we performed the inhibition
285 assay on nutrient agar plates. The sub-inhibitory concentration of daptomycin (2.5 µg/ml) used
286 in liquid culture was toxic to the cells on agar plates (Fig. S8E), so we lowered the daptomycin

287 concentration to 0.5 $\mu\text{g/ml}$ to prevent drug toxicity in the agar-based antagonism assay. Plating
288 T7SS producing *E. faecalis* OG1RF cells and *E. faecalis* Δpip_{V583} bystander cells at a ratio of
289 10:1 resulted in ~10-fold inhibition of bystander growth (Fig. 3E). Although 0.5 $\mu\text{g/ml}$ of
290 daptomycin did not dramatically increase *E. faecalis* OG1RF T7SS transcript abundances, this
291 was sufficient to promote daptomycin mediated T7SS inhibition of bystanders on agar plates
292 (Fig. 3E and Fig. S8E). These data show that in addition to phages, antibiotics can be sensed
293 by *E. faecalis* thereby inducing T7SS antagonism of non-kin bacterial cells. These data also
294 show that the magnitude of T7SS gene expression and forcing bacteria-bacteria contact is
295 directly related to the potency of T7SS inhibition.

296

297 **The primary bile acid sodium cholate does not modulate *E. faecalis* T7SS gene** 298 **expression**

299 To gain insight into host-associated environmental cues that could trigger *E. faecalis*
300 OG1RF T7SS, we measured T7SS transcription in the presence of a sub-inhibitory
301 concentration of the primary bile acid sodium cholate, an abundant compound found in the
302 mammalian intestinal tract and that is known to promote bacterial cell membrane stress [57, 58].
303 4% sodium cholate, a concentration that has been shown to severely impair the growth of *E.*
304 *faecalis* OG1RF cell envelop mutants, caused only a minor reduction in cell density of wild type
305 *E. faecalis* OG1RF [59] (Fig. S9A) and it did not stimulate T7SS gene expression (Fig. S9B).
306 Collectively, these data show that T7SS induction in *E. faecalis* occurs in response to select cell
307 envelope stressors.

308

309 **IreK and OG1RF_11099 facilitate T7SS expression in phage infected *E. faecalis* OG1RF** 310 **via a non-canonical signaling pathway**

311 Having established that both phage and daptomycin mediated membrane damage
312 independently stimulates heightened *E. faecalis* OG1RF T7SS gene expression and

313 antagonistic activity, we next sought to identify the genetic determinants that sense this damage
314 and promote T7SS transcription. Two-component systems, LiaR/S and CroS/R, and the PASTA
315 kinase family protein IreK are well-characterized modulators of enterococcal cell envelope
316 homeostasis and antimicrobial tolerance [60-62]. Aberrant cardiolipin microdomain remodeling
317 in the bacterial cell membrane in the absence of the LiaR response regulator results in
318 daptomycin hypersensitivity and virulence attenuation [63]. CroS/R signaling and subsequent
319 modulation of gene expression govern cell wall integrity and promote resistance to
320 cephalosporins, glycopeptides and beta—lactam antibiotics [64-66]. The *ireK* encoded
321 transmembrane Ser/Thr kinase regulates cell wall homeostasis, antimicrobial resistance, and
322 contributes to bacterial fitness during long-term colonization of the intestinal tract [61, 67, 68].
323 Recently it has been shown that direct cross-talk between IreK and the CroS/R system
324 positively impacts enterococcal cephalosporin resistance [69].

325 Wild type *E. faecalis* OG1RF, an *ireK* in-frame deletion mutant [61] and transposon (Tn)
326 insertion mutants of *liaR*, *liaS*, *croR*, and *croS* [70] all display similar growth kinetics in the
327 absence of phage VPE25 infection (Fig. S10A). Although *croR*-Tn and *croS*-Tn exhibit
328 reductions in the plaquing efficiency of VPE25 particles, none of these genetic elements of
329 enterococcal cell wall homeostasis and antibiotic resistance were required for VPE25 infection
330 (Fig. S10B). We queried the expression levels of T7SS genes in these isogenic mutants during
331 phage VPE25 infection (MOI = 1). T7SS gene expression was not enhanced in the $\Delta ireK$ mutant
332 during phage infection (Fig. 4A), whereas *liaR*-Tn, *liaS*-Tn, *croR*-Tn, and *croS*-Tn produced
333 heightened levels of T7SS transcripts similar to the wild type *E. faecalis* OG1RF compared to
334 the uninfected controls (Fig. S11A – S11F). A sub-lethal concentration of the cephalosporin
335 ceftriaxone did not induce T7SS gene expression (Fig. S12A), indicating that expression of
336 T7SS genes following phage mediated membrane damage signals through a pathway that is
337 distinct from the IreK response to cephalosporin stress. Additionally, the $\Delta ireK$ mutant
338 phenocopies the $\Delta essB$ mutant strain in the interbacterial antagonism co-culture assay, wherein

339 the $\Delta ireK$ mutant is unable to mediate phage induced T7SS dependent killing of the phage
340 resistant *E. faecalis* Δpip_{V583} non-kin cells (Fig. 4B). T7SS antagonism is restored in *E. faecalis*
341 $\Delta ireK$ by introducing the wild type gene in *trans* (Fig. 4B). Collectively, these results indicate that
342 IreK senses phage mediated membrane damage promoting T7SS transcription independent of
343 the CroS/R pathway.

344 OG1RF_11099, located immediately upstream of the T7SS cluster is predicted to encode a
345 GntR family transcriptional regulator, thus we sought to assess the contribution of
346 OG1RF_11099 on T7SS transcription and functionality. *E. faecalis* OG1RF carrying a
347 transposon insertion in OG1RF_11099 is equally susceptible to phage VPE25 infection
348 compared to wild type *E. faecalis* OG1RF (Fig. S2A) In contrast to wild type *E. faecalis* OG1RF,
349 T7SS genes were not induced during phage predation of *E. faecalis* OG1RF_11099-Tn (Fig.
350 4C). We evaluated the influence of OG1RF_11099-dependent regulation on the activity of T7SS
351 in intraspecies antagonism using our co-culture assay. Similar to *E. faecalis* $\Delta essB$, the
352 OG1RF_11099-Tn mutant displayed attenuated T7SS activity in phage infected co-cultures
353 (Fig. 4D). T7SS dependent antagonism of *E. faecalis* OG1RF_11099-Tn could be restored
354 following complementation (Fig. 4D). Collectively, these results indicate that *OG1RF_11099*
355 encodes a positive regulator of *E. faecalis* T7SS important for phage mediated inhibition of
356 bystander bacteria. Given that IreK governs downstream signaling events via phosphorylation
357 [71], and the fact that OG1RF_11099 was not differentially expressed in response to phage
358 infection of wild type *E. faecalis* OG1RF or *ireK* mutant strains (Fig. S12B), suggests that either
359 post-translational modification of OG1RF_11099 or a yet unidentified protein downstream of
360 IreK engaging with OG1RF_11099 accounts for T7SS gene expression during phage infection.

361

362 Discussion

363 Despite the fact that bacteria exist in complex microbial communities that socially interact
364 [72, 73], phage predation studies have primarily been performed in monoculture [24, 74-76].

365 Studies report phage-mediated effects on non-target bacteria linked to interbacterial interactions
366 and evolved phage tropism for non-cognate bacteria [77-79], whereas other studies have
367 identified minimal changes in microbiota diversity during phage therapy [77, 80].

368 Our results extend previous work that observed the induction of *E. faecalis* OG1RF T7SS
369 gene expression in response to phage infection [24]. By using an *in vitro* antibacterial
370 antagonism assay, we discovered that phage predation of *E. faecalis* OG1RF has an inhibitory
371 effect on non-phage targeted bacterial species during co-culture. Our work shows that phage
372 mediated inhibition of Gram positive bystander bacteria relies on the expression and activity of
373 T7SS genes. This work establishes a framework to begin investigating if and how phage
374 infection of target bacteria influences non-target bacterial populations in complex communities
375 such as the microbiota.

376 Our data suggest that membrane stress associated with phage infection or sub-lethal
377 daptomycin treatment stimulates T7SS mediated antibacterial antagonism of *E. faecalis* OG1RF
378 (Fig. 5). Given that daptomycin is used to target vancomycin-resistant enterococcal infections,
379 this finding provides a hypothesis for how antibiotic-resistant enterococci achieve overgrowth
380 and dominate the microbiota following antibiotic treatment. Further investigation is required to
381 understand how T7SS induction might contribute to enterococcal fitness in polymicrobial
382 environments. Although exposure to a sub-inhibitory level of primary bile salt (a common
383 molecule found in the intestine) did not elicit T7SS expression, it is possible that other stressors
384 encountered in the intestinal tract, including lysozyme, antimicrobial proteins, and nutrient
385 availability could influence T7SS activity in *E. faecalis*. Indeed, *E. faecalis* T7SS mutants are
386 defective in their ability to colonize the murine reproductive tract, which like the intestine is a
387 polymicrobial environment [36].

388 We discovered that transcriptional activation of the T7SS during phage infection relies on
389 IreK (Fig. 5). Previously characterized IreK-mediated stress response pathways, including
390 cephalosporin stress or CroS/R signaling, did not contribute to T7SS expression. We

391 hypothesize that IreK senses diverse environmental stressors and coordinates distinct outputs
392 in response to specific stimuli. Considering that IreK signaling is important for *E. faecalis*
393 intestinal colonization [68], it is possible that IreK-dependent T7SS expression in response to
394 intestinal cues modulate interbacterial interactions and enterococcal persistence in the intestine.
395 However, the molecular mechanism by which IreK facilitates T7SS transcription remains
396 unanswered. Additionally, we currently do not know if IreK directly senses phage or daptomycin
397 mediated membrane damage or some other signal feeds into IreK to facilitate T7SS induction.

398 Additionally, we discovered that *E. faecalis* OG1RF T7SS transcription is regulated by a
399 GntR-family transcriptional regulator encoded by OG1RF_11099, a gene found immediately
400 upstream of the T7SS cluster (Fig. 5). Interestingly, OG1RF_11099 is highly conserved across
401 enterococci, including *E. faecalis* V583 (Fig. 1A) and other strains that lack T7SS. The presence
402 of a conserved transcriptional regulator in the absence of its target genetic region supports the
403 idea that certain strains of enterococci have undergone genome reduction as an evolutionary
404 strategy to adapt to unique host and non-host environments. It is possible that in *E. faecalis*
405 V583, the OG1RF_11099 homolog (EF1328) has been retained to regulate other genes within
406 the regulon that are less dispensable than T7SS. Additionally, our data indicate that
407 OG1RF_11099 transcription is not dependent on IreK or and is not induced during phage
408 infection of wild type *E. faecalis* OG1RF. Previously published work demonstrated that IreK
409 kinase activity is essential for driving the cell wall stress response in *E. faecalis* [67, 71].
410 Therefore, we hypothesize that IreK directly or indirectly regulates OG1RF_11099 activity for
411 T7SS expression via post-translational modification.

412 Antibacterial properties of T7SS substrates have been demonstrated [26, 27, 40]. Here we
413 provide evidence that mutation in the LXG toxin encoded by OG1RF_11121 abrogates phage
414 induced T7SS dependent inhibition of bystander bacteria while expression of the downstream
415 immunity gene OG1RF_11122 in T7SS targeted *E. faecalis* Δpip_{V583} cells conferred partial
416 protection from this inhibition. It is possible that constitutive expression of OG1RF_11122 from a

417 multicopy plasmid results in elevated accumulation of OG1RF_11122 in the bystander strain
418 which is toxic and could account for the partial protection phenotype. Aside from its LXG
419 domain, OG1RF_11121 does not harbor any other recognizable protein domains, hence the
420 mechanism underlying its toxicity is unclear. Whitney *et al.* demonstrated that LXG toxin
421 antagonism is contact-dependent, having minimal to no impact on target cells in liquid media
422 [27]. Although we found that physical engagement is crucial for *E. faecalis* T7SS mediated
423 antagonism, we observed a significant reduction in target cell growth in liquid media both during
424 phage and daptomycin treatment of T7SS proficient *E. faecalis*.

425 In contrast to the broad antagonism of *S. intermedius* T7SS [27], the *E. faecalis* OG1RF
426 T7SS targets a more limited number of bacterial species. Interestingly, *E. faecalis* OG1RF T7SS
427 antagonism is ineffective against various species of streptococci, which like the enterococci are
428 lactic acid bacteria. Nucleotide- and protein-based homology searches did not reveal
429 homologs of candidate immunity proteins, OG1RF_11110, OG1RF_11112, OG1RF_11122, or
430 OG1RF_12413, in *S. agalactiae* COH1. Genome sequences of the other four streptococci used
431 in this present study are not available, and hence we cannot comment on the presence of
432 potential immunity proteins against OG1RF T7SS toxins in these strains. However, resistance of
433 multiple streptococcal species to OG1RF T7SS mediated inhibition suggest that common cell
434 surface modifications, e.g., capsule or surface polysaccharides, might be responsible for
435 blocking toxin activity. Narrow target range is a common attribute of contact-dependent toxins
436 that interact with specific membrane receptors on target cells to exert inhibitory activity [81].
437 However, specific receptors of T7SS toxins are yet to be identified. It is possible that specific or
438 non-specific interactions between the *E. faecalis* OG1RF and *S. aureus* or *L. monocytogenes*
439 cell surfaces facilitate T7SS interbacterial antagonism and such interactions are incompatible or
440 occluded for the streptococci.

441 It is currently unknown whether T7SS toxin delivery requires contact with a receptor on
442 target cells or whether delivery can occur in the absence of a receptor. Examples of both

443 methods of toxin delivery are widespread in bacteria. Toxins such as colicins and R-pyocins
444 mediate contact with target cells via protein receptors and LPS, respectively [82-84]. Delivery of
445 colicins and toxins produced by contact-dependent inhibition systems in Gram-negative bacteria
446 requires interactions with receptors at the outer and inner membranes [85, 86]. Conversely, the
447 T6SS needle-like machinery that punctures target cell envelopes delivers toxins in a contact-
448 dependent, receptor-independent manner [87]. Cell surface moieties can also affect recognition
449 of target cells and subsequent toxin delivery. The presence of capsule can block target cell
450 recognition by contact-dependent growth inhibition systems in *Acinetobacter baumannii* [88], *E.*
451 *coli* [89] and *Klebsiella pneumoniae* [90]. Therefore, it is possible that a feature of the
452 streptococcal cell surface, such as capsule modifications, renders them insensitive to killing by
453 toxins delivered by the *E. faecalis* OG1RF T7SS.

454 Enterococci occupy polymicrobial infections often interacting with other bacteria [91-94].
455 Although commensal *E. faecalis* antagonize virulent *S. aureus* through the production of
456 superoxide [95], the two species also exhibit growth synergy via exchange of critical nutrients
457 [96]. Here, we show that phage treatment of *E. faecalis* OG1RF can indirectly impact the growth
458 of neighboring phage-resistant bacteria, including *S. aureus*, in a T7SS-dependent manner,
459 suggesting that phage therapy directed against enterococci and driving T7SS activity could be
460 useful for the treatment of polymicrobial infections. However, the counter argument is that
461 phage therapy directed against enterococci could push a bacterial community toward dysbiosis,
462 as phage induced T7SS activity could directly inhibit beneficial bystander bacteria. This raises
463 questions about the consequences of phage mediated off-target effects on bacteria. Could
464 phage induced T7SS activity be used to reduce phage expansion into other closely related
465 strains as a means to dilute phages out of a population, or is it simply that phage induction of
466 the T7SS serves as a mechanism that benefits a select few within a population to aid in their
467 reoccupation of a niche upon overcoming phage infection? Future studies aimed at exploring

468 enterococcal T7SS antagonism in polymicrobial communities should help elucidate the impact
469 of phages on microbial community composition.

470

471 **Materials and Methods**

472 **Bacteria and bacteriophages.** Bacteria and phages used in this study are listed in Table S1.

473 Bacteria were grown with aeration in Todd-Hewitt broth (THB) or on THB agar supplemented

474 with 10mM MgSO₄ at 37°C. The following antibiotic concentrations were added to media for the

475 selection of specific bacterial strains or species: *E. faecalis* OG1RF (25 µg/ml fusidic acid, 50

476 µg/ml rifampin), *E. faecalis* V583 Δpip_{V583} (25 µg/ml or 100 µg/ml gentamicin in liquid and agar

477 media, respectively), *S. aureus* AH2146 LAC $\Phi 11:LL29$ (1 µg/ml tetracycline), *L.*

478 *monocytogenes* 10403S (100 µg/ml streptomycin), *S. gordonii* ATCC 49818 (500 µg/ml

479 streptomycin), *S. salivarius* K12 (100 µg/ml spectinomycin), *V. cholerae* C6706 int I4::TnFL63

480 and *S. enterica* serovar Typhimurium 140285 put::Kan (50 µg/ml kanamycin). *S. agalactiae*

481 COH1 was distinguished from *E. faecalis* on Chrome indicator Agar (CHROMagar StrepB

482 SB282). We were unable to differentially select *E. coli*, *L. lactis*, *S. pyogenes* and *S. mitis* from

483 *E. faecalis* based on antibiotic sensitivity. Therefore, colony counts of these bacteria in co-

484 culture experiments were acquired by subtracting the *E. faecalis* colony numbers on selective

485 media from the total number of colonies on non-selective media. Strains harboring pLZ12A and

486 its derivatives were grown in the presence of 20 µg/ml chloramphenicol and strains carrying

487 pCIEtm and pCIEtm derivatives were selected on media containing 5 µg/ml tetracycline.

488

489 **Bioinformatic analyses.** Genome sequences of *E. faecalis* V583 (NC_004668.1) and OG1RF

490 (NC_017316.1) were obtained from NCBI. Alignments were generated and visualized using

491 EasyFig [97]. OG1RF protein domains were identified using KEGG [98] and ExPASy PROSITE

492 [99]. Structure modeling of OG1RF_12414 was done with Phyre2 [48]. Crystal structures

493 overlays were generated using Pymol [100]. The EsxA phylogenetic tree was constructed in

494 MEGA version X [101] using non-redundant protein sequences obtained from NCBI BLAST
495 [102] with OG1RF_11100 as input and was edited using the Interactive Tree Of Life browser
496 [103]. OG1RF_11109 was used as an input for the NCBI Conserved Domain Architecture
497 Retrieval Tool [104] to identify protein domains that co-occur with LXG domains in *Enterococcus*
498 (NCBI:txid1350).

499

500 **Antibiotic sensitivity profiles.** Antibiotic susceptibility profiles for ampicillin, vancomycin, and
501 daptomycin were determined using a broth microdilution assay. Overnight (O/N) *E. faecalis*
502 OG1RF cultures were diluted to 5×10^6 CFU/ml and 100 μ l was added to each well of a 96-
503 well plate to give a final cell density of 5×10^5 CFU/ml. Antibiotic stocks were added to the
504 first column of each row, mixed thoroughly, and serially diluted 2-fold across the rows. The last
505 column was used as a no drug control. Cultures containing daptomycin were supplemented with
506 50 μ g/ml CaCl_2 . Bacterial growth was monitored by measuring absorbance (OD_{600}) using a
507 Synergy H1 microplate reader set to 37°C with continuous shaking O/N. Growth curves are
508 presented as the average of three biological replicates. A concentration of antibiotic just below
509 the drug amount that inhibits bacterial growth was deemed sub-lethal and used to examine
510 T7SS genes expression.

511

512 **Co-culture bacterial antagonism assays.** For inter- and intraspecies antagonism assays in
513 liquid media, O/N cultures of different bacteria were diluted in THB containing 10mM MgSO_4 to
514 an OD_{600} of 0.2 and mixed together in a 1:1 or 10:1 ratio. The mixed cell suspensions were
515 either left untreated or treated with phage VPE25 (MOI 0.01) or daptomycin (2.5 μ g/ml) and
516 grown at 37°C with aeration. For pheromone induction of genes OG1RF_11121, *ireK* and
517 OG1RF_11099 cloned into pCIETm, 10 ng/ml cCF10 (from Mimotopes) was added at the time of
518 phage administration. For antagonism experiments on agar plates, O/N cultures of different
519 strains were diluted to an OD_{600} of 0.2 and mixed together in a 1:1 or 10:1 ratio. A total of 10^7

520 cells from mixed culture suspension was added to 5 ml THB + 0.35% agar at 55°C and were
521 poured over the surface of a THB agar plate in the absence or presence of daptomycin (0.5
522 µg/ml). The plates were incubated at 37°C under static conditions for 24 hours. Cells were
523 harvested by scraping off the top agar, resuspending in 5 ml of PBS, and the cfus were obtained
524 by plating serially diluted cell suspension on appropriate selective agar plates. Relative viability
525 was calculated from the ratio of target strain cfu in the treated versus the untreated co-culture.
526 The assays were performed in biological triplicates.

527

528 **RNA extraction and quantitative PCR.** RNA was extracted from phage, antibiotic, or 4%
529 sodium cholate treated or untreated *E. faecalis* OG1RF cells using an RNeasy Mini Kit (Qiagen)
530 with the following published modifications [24]. cDNA was generated from 1 µg of RNA using
531 qScript cDNA SuperMix (QuantaBio) and transcript levels were analyzed by qPCR using
532 PowerUp SYBR Green Master Mix (Applied Biosystems). Transcript abundances were
533 normalized to 16S rRNA gene transcripts and fold-change was calculated by comparing to
534 untreated controls. All data are represented as the average of three biological replicates. All the
535 primers used for qPCR are listed in Table S1.

536

537 **Bacterial growth curves.** 25 ml of 10mM MgSO₄ supplemented THB was inoculated with O/N
538 cultures of *E. faecalis* diluted to an OD₆₀₀ of 0.025 and distributed to a 96-well plate in 0.1 ml
539 volumes. Cultures were incubated at 37° C with aeration. OD₆₀₀ was measured periodically for
540 18 hours in a Synergy H1 microplate reader.

541

542 **Efficiency of plating (EOP) assays.** To investigate if phage VPE25 can infect and lyse *E.*
543 *faecalis* mutants and various other bacterial species, 10⁷ PFU/ml of phage was serially diluted
544 and the phage was titered on each strain using a THB agar overlay plaque assay. EOP is

545 expressed as the percentage of phage titer from each strain relative to the wild type *E. faecalis*
546 OG1RF control. Data are presented as the average of three biological replicates.

547

548 **Construction of *E. faecalis* mutants and complementation.** Isolation of *E. faecalis* genomic
549 DNA was performed using a ZymoBIOMICS DNA Miniprep Kit (Zymo Research). All PCR used
550 for cloning were performed with high fidelity KOD Hot Start DNA Polymerase (EMD Millipore). *E.*
551 *faecalis* Δ *essB* was generated by allelic replacement by cloning an in frame *essB* deletion
552 product into pLT06 using Gibson Assembly® Master Mix (New England Biolabs), integrating this
553 construct into the chromosome, and resolving the deletion mutant by homologous
554 recombination [105-107]. For ectopic expression of putative immunity proteins, coding regions
555 of OG1RF_11110, OG1RF_11112, OG1RF_11122, and OG1RF_12413 were cloned
556 downstream of the *bacA* promoter (P_{bacA}) by restriction digestion and ligation into the shuttle
557 vector pLZ12A [20]. Coding regions of *ireK* and OG1RF_11099 were cloned downstream of the
558 cCF10 responsive promoter (P_Q) by restriction digestion and ligation into pCIE and pCIEtm
559 vectors, respectively. As attempts to clone OG1RF_11121 by itself were unsuccessful, we
560 cloned the OG1RF_11121 and OG1RF_11122 open reading frames, which overlap by 13 base
561 pairs, together under the P_Q promoter in pCIEtm plasmid. Primer sequences and restriction
562 enzymes used for cloning are listed in Table S1. Plasmids were introduced into
563 electrocompetent *E. faecalis* cells as previously described [20].

564

565 **Statistical analysis.** Statistical tests were performed using GraphPad – Prism version 8.2.1.
566 For qPCR and bacterial competition assays, unpaired Student's t-tests were used. *P* values are
567 indicated in the figure legends.

568

569 **Data availability.** All raw data are available upon request.

570

571 **References**

- 572 1. Lebreton F, Willems RJL, Gilmore MS. *Enterococcus* diversity, origins in nature, and gut
573 colonization. In: Gilmore MS, Clewell DB, Ike Y, Shankar N, editors. Enterococci: from
574 commensals to leading causes of drug resistant infection. Boston2014.
- 575 2. Onderdonk AB, Bartlett JG, Louie T, Sullivan-Seigler N, Gorbach SL. Microbial synergy
576 in experimental intra-abdominal abscess. *Infect Immun*. 1976;13(1):22-6. Epub 1976/01/01.
577 PubMed PMID: 814099; PubMed Central PMCID: PMC420571.
- 578 3. Weiner-Lastinger LM, Abner S, Edwards JR, Kallen AJ, Karlsson M, Magill SS, et al.
579 Antimicrobial-resistant pathogens associated with adult healthcare-associated infections:
580 Summary of data reported to the National Healthcare Safety Network, 2015-2017. *Infect Control
581 Hosp Epidemiol*. 2020;41(1):1-18. Epub 2019/11/27. doi: 10.1017/ice.2019.296. PubMed PMID:
582 31767041.
- 583 4. Arias CA, Panesso D, McGrath DM, Qin X, Mojica MF, Miller C, et al. Genetic basis for
584 *in vivo* daptomycin resistance in enterococci. *N Engl J Med*. 2011;365(10):892-900. Epub
585 2011/09/09. doi: 10.1056/NEJMoa1011138. PubMed PMID: 21899450; PubMed Central
586 PMCID: PMC3205971.
- 587 5. Liu Y, Wang Y, Wu C, Shen Z, Schwarz S, Du XD, et al. First report of the multidrug
588 resistance gene *cf*r in *Enterococcus faecalis* of animal origin. *Antimicrob Agents Chemother*.
589 2012;56(3):1650-4. Epub 2011/12/29. doi: 10.1128/AAC.06091-11. PubMed PMID: 22203597;
590 PubMed Central PMCID: PMC3294887.
- 591 6. Patel SN, Memari N, Shahinas D, Toye B, Jamieson FB, Farrell DJ. Linezolid resistance
592 in *Enterococcus faecium* isolated in Ontario, Canada. *Diagn Microbiol Infect Dis*.

593 2013;77(4):350-3. Epub 2013/10/08. doi: 10.1016/j.diagmicrobio.2013.08.012. PubMed PMID:
594 24095643.

595 7. Ubeda C, Taur Y, Jenq RR, Equinda MJ, Son T, Samstein M, et al. Vancomycin-
596 resistant *Enterococcus* domination of intestinal microbiota is enabled by antibiotic treatment in
597 mice and precedes bloodstream invasion in humans. *J Clin Invest*. 2010;120(12):4332-41. Epub
598 2010/11/26. doi: 10.1172/JCI43918. PubMed PMID: 21099116; PubMed Central PMCID:
599 PMCPMC2993598.

600 8. Zirakzadeh A, Patel R. Vancomycin-resistant enterococci: colonization, infection,
601 detection, and treatment. *Mayo Clin Proc*. 2006;81(4):529-36. Epub 2006/04/14. doi:
602 10.4065/81.4.529. PubMed PMID: 16610573.

603 9. Taur Y, Xavier JB, Lipuma L, Ubeda C, Goldberg J, Gobourne A, et al. Intestinal
604 domination and the risk of bacteremia in patients undergoing allogeneic hematopoietic stem cell
605 transplantation. *Clin Infect Dis*. 2012;55(7):905-14. Epub 2012/06/22. doi: 10.1093/cid/cis580.
606 PubMed PMID: 22718773; PubMed Central PMCID: PMCPMC3657523.

607 10. Munoz-Price LS, Lolans K, Quinn JP. Emergence of resistance to daptomycin during
608 treatment of vancomycin-resistant *Enterococcus faecalis* infection. *Clin Infect Dis*.
609 2005;41(4):565-6. Epub 2005/07/20. doi: 10.1086/432121. PubMed PMID: 16028170.

610 11. Palmer KL, Daniel A, Hardy C, Silverman J, Gilmore MS. Genetic basis for daptomycin
611 resistance in enterococci. *Antimicrob Agents Chemother*. 2011;55(7):3345-56. Epub
612 2011/04/20. doi: 10.1128/AAC.00207-11. PubMed PMID: 21502617; PubMed Central PMCID:
613 PMCPMC3122436.

614 12. Jasni AS, Mullany P, Hussain H, Roberts AP. Demonstration of conjugative transposon
615 (Tn5397)-mediated horizontal gene transfer between *Clostridium difficile* and *Enterococcus*

- 616 *faecalis*. Antimicrob Agents Chemother. 2010;54(11):4924-6. Epub 2010/08/18. doi:
617 10.1128/AAC.00496-10. PubMed PMID: 20713671; PubMed Central PMCID:
618 PMCPMC2976158.
- 619 13. Palmer KL, Kos VN, Gilmore MS. Horizontal gene transfer and the genomics of
620 enterococcal antibiotic resistance. Curr Opin Microbiol. 2010;13(5):632-9. Epub 2010/09/15. doi:
621 10.1016/j.mib.2010.08.004. PubMed PMID: 20837397; PubMed Central PMCID:
622 PMCPMC2955785.
- 623 14. Chang S, Sievert DM, Hageman JC, Boulton ML, Tenover FC, Downes FP, et al.
624 Infection with vancomycin-resistant *Staphylococcus aureus* containing the *vanA* resistance
625 gene. N Engl J Med. 2003;348(14):1342-7. Epub 2003/04/04. doi: 10.1056/NEJMoa025025.
626 PubMed PMID: 12672861.
- 627 15. Kurenbach B, Bohn C, Prabhu J, Abudukerim M, Szewzyk U, Grohmann E. Intergeneric
628 transfer of the *Enterococcus faecalis* plasmid pIP501 to *Escherichia coli* and *Streptomyces*
629 *lividans* and sequence analysis of its *tra* region. Plasmid. 2003;50(1):86-93. Epub 2003/06/27.
630 PubMed PMID: 12826062.
- 631 16. Kortright KE, Chan BK, Koff JL, Turner PE. Phage therapy: a renewed approach to
632 combat antibiotic-resistant bacteria. Cell Host Microbe. 2019;25(2):219-32. Epub 2019/02/15.
633 doi: 10.1016/j.chom.2019.01.014. PubMed PMID: 30763536.
- 634 17. Cheng M, Liang J, Zhang Y, Hu L, Gong P, Cai R, et al. The bacteriophage EF-P29
635 efficiently protects against lethal vancomycin-resistant *Enterococcus faecalis* and alleviates gut
636 microbiota imbalance in a murine bacteremia model. Front Microbiol. 2017;8:837. Epub
637 2017/05/26. doi: 10.3389/fmicb.2017.00837. PubMed PMID: 28536572; PubMed Central
638 PMCID: PMCPMC5423268.

- 639 18. Gelman D, Beyth S, Lerer V, Adler K, Poradosu-Cohen R, Coppenhagen-Glazer S, et al.
640 Combined bacteriophages and antibiotics as an efficient therapy against VRE *Enterococcus*
641 *faecalis* in a mouse model. Res Microbiol. 2018;169(9):531-9. Epub 2018/05/20. doi:
642 10.1016/j.resmic.2018.04.008. PubMed PMID: 29777835.
- 643 19. Uchiyama J, Rashel M, Takemura I, Wakiguchi H, Matsuzaki S. *In silico* and *in vivo*
644 evaluation of bacteriophage phiEF24C, a candidate for treatment of *Enterococcus faecalis*
645 infections. Appl Environ Microbiol. 2008;74(13):4149-63. Epub 2008/05/06. doi:
646 10.1128/AEM.02371-07. PubMed PMID: 18456848; PubMed Central PMCID:
647 PMCPMC2446516.
- 648 20. Chatterjee A, Johnson CN, Luong P, Hullahalli K, McBride SW, Schubert AM, et al.
649 Bacteriophage resistance alters antibiotic-mediated intestinal expansion of enterococci. Infect
650 Immun. 2019;87(6):e00085-19. Epub 2019/04/03. doi: 10.1128/IAI.00085-19. PubMed PMID:
651 30936157; PubMed Central PMCID: PMCPMC6529655.
- 652 21. Lin DM, Koskella B, Lin HC. Phage therapy: an alternative to antibiotics in the age of
653 multi-drug resistance. World J Gastrointest Pharmacol Ther. 2017;8(3):162-73. Epub
654 2017/08/23. doi: 10.4292/wjgpt.v8.i3.162. PubMed PMID: 28828194; PubMed Central PMCID:
655 PMCPMC5547374.
- 656 22. Loc-Carrillo C, Abedon ST. Pros and cons of phage therapy. Bacteriophage.
657 2011;1(2):111-4. Epub 2012/02/16. doi: 10.4161/bact.1.2.14590. PubMed PMID: 22334867;
658 PubMed Central PMCID: PMCPMC3278648.
- 659 23. Wu S, Zachary E, Wells K, Loc-Carrillo C. Phage Therapy: future inquiries. Postdoc J.
660 2013;1(6):24-35. Epub 2013/06/01. PubMed PMID: 28286802; PubMed Central PMCID:
661 PMCPMC5342839.

- 662 24. Chatterjee A, Willett JLE, Nguyen UT, Monogue B, Palmer KL, Dunny GM, et al. Parallel
663 Genomics Uncover Novel Enterococcal-Bacteriophage Interactions. *mBio*. 2020;11(2). Epub
664 2020/03/05. doi: 10.1128/mBio.03120-19. PubMed PMID: 32127456; PubMed Central PMCID:
665 PMCPMC7064774.
- 666 25. Unnikrishnan M, Constantinidou C, Palmer T, Pallen MJ. The enigmatic Esx proteins:
667 looking beyond mycobacteria. *Trends Microbiol*. 2017;25(3):192-204. Epub 2016/11/30. doi:
668 10.1016/j.tim.2016.11.004. PubMed PMID: 27894646.
- 669 26. Cao Z, Casabona MG, Kneuper H, Chalmers JD, Palmer T. The type VII secretion
670 system of *Staphylococcus aureus* secretes a nuclease toxin that targets competitor bacteria.
671 *Nat Microbiol*. 2016;2:16183. Epub 2016/10/11. doi: 10.1038/nmicrobiol.2016.183. PubMed
672 PMID: 27723728; PubMed Central PMCID: PMCPMC5325307.
- 673 27. Whitney JC, Peterson SB, Kim J, Pazos M, Verster AJ, Radey MC, et al. A broadly
674 distributed toxin family mediates contact-dependent antagonism between Gram-positive
675 bacteria. *Elife*. 2017;6. Epub 2017/07/12. doi: 10.7554/eLife.26938. PubMed PMID: 28696203;
676 PubMed Central PMCID: PMCPMC5555719.
- 677 28. Burts ML, DeDent AC, Missiakas DM. EsaC substrate for the ESAT-6 secretion pathway
678 and its role in persistent infections of *Staphylococcus aureus*. *Mol Microbiol*. 2008;69(3):736-46.
679 Epub 2008/06/17. doi: 10.1111/j.1365-2958.2008.06324.x. PubMed PMID: 18554323; PubMed
680 Central PMCID: PMCPMC2597432.
- 681 29. Ishii K, Adachi T, Yasukawa J, Suzuki Y, Hamamoto H, Sekimizu K. Induction of
682 virulence gene expression in *Staphylococcus aureus* by pulmonary surfactant. *Infect Immun*.
683 2014;82(4):1500-10. Epub 2014/01/24. doi: 10.1128/IAI.01635-13. PubMed PMID: 24452679;
684 PubMed Central PMCID: PMCPMC3993393.

- 685 30. Lopez MS, Tan IS, Yan D, Kang J, McCreary M, Modrusan Z, et al. Host-derived fatty
686 acids activate type VII secretion in *Staphylococcus aureus*. Proc Natl Acad Sci U S A.
687 2017;114(42):11223-8. Epub 2017/10/05. doi: 10.1073/pnas.1700627114. PubMed PMID:
688 28973946; PubMed Central PMCID: PMC5651732.
- 689 31. Tchoupa AK, Watkins KE, Jones RA, Kuroki A, Alam MT, Perrier S, et al. The type VII
690 secretion system protects *Staphylococcus aureus* against antimicrobial host fatty acids. bioRxiv.
691 2020:572172. doi: 10.1101/572172.
- 692 32. Bourgogne A, Garsin DA, Qin X, Singh KV, Sillanpaa J, Yerrapragada S, et al. Large
693 scale variation in *Enterococcus faecalis* illustrated by the genome analysis of strain OG1RF.
694 Genome Biol. 2008;9(7):R110. Epub 2008/07/10. doi: 10.1186/gb-2008-9-7-r110. PubMed
695 PMID: 18611278; PubMed Central PMCID: PMC530867.
- 696 33. Paulsen IT, Banerjee L, Myers GS, Nelson KE, Seshadri R, Read TD, et al. Role of
697 mobile DNA in the evolution of vancomycin-resistant *Enterococcus faecalis*. Science.
698 2003;299(5615):2071-4. Epub 2003/03/29. doi: 10.1126/science.1080613. PubMed PMID:
699 12663927.
- 700 34. Reiter WD, Palm P, Yeats S. Transfer RNA genes frequently serve as integration sites
701 for prokaryotic genetic elements. Nucleic Acids Res. 1989;17(5):1907-14. doi:
702 10.1093/nar/17.5.1907. PubMed PMID: 2467253; PubMed Central PMCID: PMC317532.
- 703 35. Lebreton F, Manson AL, Saavedra JT, Straub TJ, Earl AM, Gilmore MS. Tracing the
704 enterococci from paleozoic origins to the hospital. Cell. 2017;169(5):849-61 e13. Epub
705 2017/05/16. doi: 10.1016/j.cell.2017.04.027. PubMed PMID: 28502769; PubMed Central
706 PMCID: PMC5499534.

- 707 36. Alhajar N, Chatterjee A, Spencer BL, Burcham LR, Willett JLE, Dunny GM, et al.
708 Genome-wide mutagenesis identifies factors involved in *Enterococcus faecalis* vaginal
709 adherence and persistence. *Infection and Immunity*. 2020:IAI.00270-20. doi: 10.1128/iai.00270-
710 20.
- 711 37. Das C, Ghosh TS, Mande SS. *In silico* dissection of type VII secretion system
712 components across bacteria: new directions towards functional characterization. *J Biosci*.
713 2016;41(1):133-43. Epub 2016/03/08. doi: 10.1007/s12038-016-9599-8. PubMed PMID:
714 26949095.
- 715 38. Burts ML, Williams WA, DeBord K, Missiakas DM. EsxA and EsxB are secreted by an
716 ESAT-6-like system that is required for the pathogenesis of *Staphylococcus aureus* infections.
717 *Proc Natl Acad Sci U S A*. 2005;102(4):1169-74. Epub 2005/01/20. doi:
718 10.1073/pnas.0405620102. PubMed PMID: 15657139; PubMed Central PMCID:
719 PMCPMC545836.
- 720 39. Duerkop BA, Huo W, Bhardwaj P, Palmer KL, Hooper LV. Molecular Basis for Lytic
721 Bacteriophage Resistance in Enterococci. *mBio*. 2016;7(4). Epub 2016/09/01. doi:
722 10.1128/mBio.01304-16. PubMed PMID: 27578757; PubMed Central PMCID:
723 PMCPMC4999554.
- 724 40. Ulhuq FR, Gomes MC, Duggan GM, Guo M, Mendonca C, Buchanan G, et al. A
725 membrane-depolarizing toxin substrate of the *Staphylococcus aureus* type VII secretion system
726 mediates intraspecies competition. *Proc Natl Acad Sci U S A*. 2020. Epub 2020/08/10. doi:
727 10.1073/pnas.2006110117. PubMed PMID: 32769205.

- 728 41. Garcia EC. Contact-dependent interbacterial toxins deliver a message. *Curr Opin*
729 *Microbiol.* 2018;42:40-6. Epub 2017/10/28. doi: 10.1016/j.mib.2017.09.011. PubMed PMID:
730 29078204; PubMed Central PMCID: PMC5899628.
- 731 42. Garcia-Bayona L, Comstock LE. Bacterial antagonism in host-associated microbial
732 communities. *Science.* 2018;361(6408). Epub 2018/09/22. doi: 10.1126/science.aat2456.
733 PubMed PMID: 30237322.
- 734 43. Zhang D, de Souza RF, Anantharaman V, Iyer LM, Aravind L. Polymorphic toxin
735 systems: comprehensive characterization of trafficking modes, processing, mechanisms of
736 action, immunity and ecology using comparative genomics. *Biol Direct.* 2012;7:18. Epub
737 2012/06/27. doi: 10.1186/1745-6150-7-18. PubMed PMID: 22731697; PubMed Central PMCID:
738 PMC3482391.
- 739 44. Klein TA, Pazos M, Surette MG, Vollmer W, Whitney JC. Molecular basis for immunity
740 protein recognition of a type VII secretion system exported antibacterial toxin. *J Mol Biol.*
741 2018;430(21):4344-58. Epub 2018/09/09. doi: 10.1016/j.jmb.2018.08.027. PubMed PMID:
742 30194969; PubMed Central PMCID: PMC6193138.
- 743 45. Jamet A, Nassif X. New players in the toxin field: polymorphic toxin systems in bacteria.
744 *mBio.* 2015;6(3):e00285-15. Epub 2015/05/07. doi: 10.1128/mBio.00285-15. PubMed PMID:
745 25944858; PubMed Central PMCID: PMC4436062.
- 746 46. Poole SJ, Diner EJ, Aoki SK, Braaten BA, t'Kint de Roodenbeke C, Low DA, et al.
747 Identification of functional toxin/immunity genes linked to contact-dependent growth inhibition
748 (CDI) and rearrangement hotspot (Rhs) systems. *PLoS Genet.* 2011;7(8):e1002217. Epub
749 2011/08/11. doi: 10.1371/journal.pgen.1002217. PubMed PMID: 21829394; PubMed Central
750 PMCID: PMC3150448.

- 751 47. Koskiniemi S, Garza-Sánchez F, Sandegren L, Webb JS, Braaten BA, Poole SJ, et al.
752 Selection of orphan Rhs toxin expression in evolved *Salmonella enterica* serovar Typhimurium.
753 PLoS Genet. 2014;10(3):e1004255. doi: 10.1371/journal.pgen.1004255. PubMed PMID:
754 24675981; PubMed Central PMCID: PMC3967940.
- 755 48. Kelley LA, Mezulis S, Yates CM, Wass MN, Sternberg MJ. The Phyre2 web portal for
756 protein modeling, prediction and analysis. Nat Protoc. 2015;10(6):845-58. Epub 2015/05/07. doi:
757 10.1038/nprot.2015.053. PubMed PMID: 25950237; PubMed Central PMCID:
758 PMCPMC5298202.
- 759 49. Wiener M, Freymann D, Ghosh P, Stroud RM. Crystal structure of colicin Ia. Nature.
760 1997;385(6615):461-4. doi: 10.1038/385461a0. PubMed PMID: 9009197.
- 761 50. Tang JY, Bullen NP, Ahmad S, Whitney JC. Diverse NADase effector families mediate
762 interbacterial antagonism via the type VI secretion system. J Biol Chem. 2018;293(5):1504-14.
763 Epub 2017/12/15. doi: 10.1074/jbc.RA117.000178. PubMed PMID: 29237732; PubMed Central
764 PMCID: PMCPMC5798281.
- 765 51. Michalska K, Quan Nhan D, Willett JLE, Stols LM, Eschenfeldt WH, Jones AM, et al.
766 Functional plasticity of antibacterial EndoU toxins. Mol Microbiol. 2018;109(4):509-27. Epub
767 2018/06/21. doi: 10.1111/mmi.14007. PubMed PMID: 29923643; PubMed Central PMCID:
768 PMCPMC6173971.
- 769 52. Zhang D, Iyer LM, Aravind L. A novel immunity system for bacterial nucleic acid
770 degrading toxins and its recruitment in various eukaryotic and DNA viral systems. Nucleic Acids
771 Res. 2011;39(11):4532-52. Epub 2011/02/11. doi: 10.1093/nar/gkr036. PubMed PMID:
772 21306995; PubMed Central PMCID: PMCPMC3113570.

- 773 53. Klein TA, Ahmad S, Whitney JC. Contact-dependent interbacterial antagonism mediated
774 by protein secretion machines. *Trends Microbiol.* 2020;28(5):387-400. Epub 2020/04/17. doi:
775 10.1016/j.tim.2020.01.003. PubMed PMID: 32298616.
- 776 54. Andersson DI, Hughes D. Microbiological effects of sublethal levels of antibiotics. *Nat*
777 *Rev Microbiol.* 2014;12(7):465-78. Epub 2014/05/28. doi: 10.1038/nrmicro3270. PubMed PMID:
778 24861036.
- 779 55. Bernier SP, Surette MG. Concentration-dependent activity of antibiotics in natural
780 environments. *Front Microbiol.* 2013;4:20. Epub 2013/02/21. doi: 10.3389/fmicb.2013.00020.
781 PubMed PMID: 23422936; PubMed Central PMCID: PMC3574975.
- 782 56. Yim G, Wang HH, Davies J. Antibiotics as signalling molecules. *Philos Trans R Soc*
783 *Lond B Biol Sci.* 2007;362(1483):1195-200. Epub 2007/03/16. doi: 10.1098/rstb.2007.2044.
784 PubMed PMID: 17360275; PubMed Central PMCID: PMC3574975.
- 785 57. Flahaut S, Frere J, Boutibonnes P, Auffray Y. Comparison of the bile salts and sodium
786 dodecyl sulfate stress responses in *Enterococcus faecalis*. *Appl Environ Microbiol.*
787 1996;62(7):2416-20. Epub 1996/07/01. doi: 10.1128/AEM.62.7.2416-2420.1996. PubMed
788 PMID: 8779581; PubMed Central PMCID: PMC168024.
- 789 58. Ridlon JM, Kang DJ, Hylemon PB. Bile salt biotransformations by human intestinal
790 bacteria. *J Lipid Res.* 2006;47(2):241-59. Epub 2005/11/22. doi: 10.1194/jlr.R500013-JLR200.
791 PubMed PMID: 16299351.
- 792 59. Dale JL, Cagnazzo J, Phan CQ, Barnes AM, Dunny GM. Multiple roles for *Enterococcus*
793 *faecalis* glycosyltransferases in biofilm-associated antibiotic resistance, cell envelope integrity,
794 and conjugative transfer. *Antimicrob Agents Chemother.* 2015;59(7):4094-105. Epub

795 2015/04/29. doi: 10.1128/AAC.00344-15. PubMed PMID: 25918141; PubMed Central PMCID:
796 PMCPMC4468649.

797 60. Kellogg SL, Kristich CJ. Functional dissection of the CroRS two-component system
798 required for resistance to cell wall stressors in *Enterococcus faecalis*. J Bacteriol.
799 2016;198(8):1326-36. Epub 2016/02/18. doi: 10.1128/JB.00995-15. PubMed PMID: 26883822;
800 PubMed Central PMCID: PMCPMC4859583.

801 61. Kristich CJ, Wells CL, Dunny GM. A eukaryotic-type Ser/Thr kinase in *Enterococcus*
802 *faecalis* mediates antimicrobial resistance and intestinal persistence. Proc Natl Acad Sci U S A.
803 2007;104(9):3508-13. Epub 2007/03/16. doi: 10.1073/pnas.0608742104. PubMed PMID:
804 17360674; PubMed Central PMCID: PMCPMC1805595.

805 62. Tran TT, Panesso D, Mishra NN, Mileykovskaya E, Guan Z, Munita JM, et al.
806 Daptomycin-resistant *Enterococcus faecalis* diverts the antibiotic molecule from the division
807 septum and remodels cell membrane phospholipids. mBio. 2013;4(4). Epub 2013/07/25. doi:
808 10.1128/mBio.00281-13. PubMed PMID: 23882013; PubMed Central PMCID:
809 PMCPMC3735187.

810 63. Reyes J, Panesso D, Tran TT, Mishra NN, Cruz MR, Munita JM, et al. A *liaR* deletion
811 restores susceptibility to daptomycin and antimicrobial peptides in multidrug-resistant
812 *Enterococcus faecalis*. J Infect Dis. 2015;211(8):1317-25. Epub 2014/11/02. doi:
813 10.1093/infdis/jiu602. PubMed PMID: 25362197; PubMed Central PMCID: PMCPMC4402337.

814 64. Comenge Y, Quintiliani R, Jr., Li L, Dubost L, Brouard JP, Hugonnet JE, et al. The
815 CroRS two-component regulatory system is required for intrinsic beta-lactam resistance in
816 *Enterococcus faecalis*. J Bacteriol. 2003;185(24):7184-92. Epub 2003/12/03. doi:

817 10.1128/jb.185.24.7184-7192.2003. PubMed PMID: 14645279; PubMed Central PMCID:
818 PMCPMC296236.

819 65. Hancock L, Perego M. Two-component signal transduction in *Enterococcus faecalis*. J
820 Bacteriol. 2002;184(21):5819-25. Epub 2002/10/11. doi: 10.1128/jb.184.21.5819-5825.2002.
821 PubMed PMID: 12374813; PubMed Central PMCID: PMCPMC135378.

822 66. Hancock LE, Perego M. Systematic inactivation and phenotypic characterization of two-
823 component signal transduction systems of *Enterococcus faecalis* V583. J Bacteriol.
824 2004;186(23):7951-8. Epub 2004/11/18. doi: 10.1128/JB.186.23.7951-7958.2004. PubMed
825 PMID: 15547267; PubMed Central PMCID: PMCPMC529088.

826 67. Kristich CJ, Little JL, Hall CL, Hoff JS. Reciprocal regulation of cephalosporin resistance
827 in *Enterococcus faecalis*. mBio. 2011;2(6):e00199-11. Epub 2011/11/03. doi:
828 10.1128/mBio.00199-11. PubMed PMID: 22045988; PubMed Central PMCID:
829 PMCPMC3202758.

830 68. Banla IL, Kommineni S, Hayward M, Rodrigues M, Palmer KL, Salzman NH, et al.
831 Modulators of *Enterococcus faecalis* cell envelope integrity and antimicrobial resistance
832 influence stable colonization of the mammalian gastrointestinal tract. Infect Immun. 2018;86(1).
833 Epub 2017/10/19. doi: 10.1128/IAI.00381-17. PubMed PMID: 29038125; PubMed Central
834 PMCID: PMCPMC5736811.

835 69. Kellogg SL, Kristich CJ. Convergence of PASTA kinase and two-component signaling in
836 response to cell wall stress in *Enterococcus faecalis*. J Bacteriol. 2018;200(12). Epub
837 2018/04/11. doi: 10.1128/JB.00086-18. PubMed PMID: 29632091; PubMed Central PMCID:
838 PMCPMC5971478.

- 839 70. Dale JL, Beckman KB, Willett JLE, Nilson JL, Palani NP, Baller JA, et al. Comprehensive
840 functional analysis of the *Enterococcus faecalis* core genome using an ordered, sequence-
841 defined collection of insertional mutations in strain OG1RF. *mSystems*. 2018;3(5). Epub
842 2018/09/19. doi: 10.1128/mSystems.00062-18. PubMed PMID: 30225373; PubMed Central
843 PMCID: PMCPMC6134198.
- 844 71. Labbe BD, Kristich CJ. Growth- and stress-induced PASTA kinase phosphorylation in
845 *Enterococcus faecalis*. *J Bacteriol*. 2017;199(21). Epub 2017/08/16. doi: 10.1128/JB.00363-17.
846 PubMed PMID: 28808126; PubMed Central PMCID: PMCPMC5626955.
- 847 72. Madsen JS, Sorensen SJ, Burmolle M. Bacterial social interactions and the emergence
848 of community-intrinsic properties. *Curr Opin Microbiol*. 2018;42:104-9. Epub 2017/12/05. doi:
849 10.1016/j.mib.2017.11.018. PubMed PMID: 29197823.
- 850 73. Xavier JB, Foster KR. Cooperation and conflict in microbial biofilms. *Proc Natl Acad Sci*
851 *U S A*. 2007;104(3):876-81. Epub 2007/01/11. doi: 10.1073/pnas.0607651104. PubMed PMID:
852 17210916; PubMed Central PMCID: PMCPMC1783407.
- 853 74. Leskinen K, Blasdel BG, Lavigne R, Skurnik M. RNA-sequencing reveals the
854 progression of phage-host interactions between phiR1-37 and *Yersinia enterocolitica*. *Viruses*.
855 2016;8(4):111. Epub 2016/04/26. doi: 10.3390/v8040111. PubMed PMID: 27110815; PubMed
856 Central PMCID: PMCPMC4848604.
- 857 75. Mojardin L, Salas M. Global transcriptional analysis of virus-host interactions between
858 phage Φ phi29 and *Bacillus subtilis*. *J Virol*. 2016;90(20):9293-304. Epub 2016/08/05. doi:
859 10.1128/JVI.01245-16. PubMed PMID: 27489274; PubMed Central PMCID: PMCPMC5044823.
- 860 76. Sacher JC, Flint A, Butcher J, Blasdel B, Reynolds HM, Lavigne R, et al. Transcriptomic
861 analysis of the *Campylobacter jejuni* response to T4-like phage NCTC 12673 infection. *Viruses*.

862 2018;10(6). Epub 2018/06/20. doi: 10.3390/v10060332. PubMed PMID: 29914170; PubMed
863 Central PMCID: PMCPMC6024767.

864 77. De Sordi L, Khanna V, Debarbieux L. The gut microbiota facilitates drifts in the genetic
865 diversity and infectivity of bacterial viruses. *Cell Host Microbe*. 2017;22(6):801-8 e3. Epub
866 2017/11/28. doi: 10.1016/j.chom.2017.10.010. PubMed PMID: 29174401.

867 78. Hsu BB, Gibson TE, Yeliseyev V, Liu Q, Lyon L, Bry L, et al. Dynamic modulation of the
868 gut microbiota and metabolome by bacteriophages in a mouse model. *Cell Host Microbe*.
869 2019;25(6):803-14 e5. Epub 2019/06/09. doi: 10.1016/j.chom.2019.05.001. PubMed PMID:
870 31175044; PubMed Central PMCID: PMCPMC6579560.

871 79. Reyes A, Wu M, McNulty NP, Rohwer FL, Gordon JI. Gnotobiotic mouse model of
872 phage-bacterial host dynamics in the human gut. *Proc Natl Acad Sci U S A*.
873 2013;110(50):20236-41. Epub 2013/11/22. doi: 10.1073/pnas.1319470110. PubMed PMID:
874 24259713; PubMed Central PMCID: PMCPMC3864308.

875 80. Dissanayake U, Ukhanova M, Moye ZD, Sulakvelidze A, Mai V. Bacteriophages reduce
876 pathogenic *Escherichia coli* counts in mice without distorting gut microbiota. *Front Microbiol*.
877 2019;10:1984. Epub 2019/09/26. doi: 10.3389/fmicb.2019.01984. PubMed PMID: 31551950;
878 PubMed Central PMCID: PMCPMC6748168.

879 81. Ruhe ZC, Wallace AB, Low DA, Hayes CS. Receptor polymorphism restricts contact-
880 dependent growth inhibition to members of the same species. *mBio*. 2013;4(4). Epub
881 2013/07/25. doi: 10.1128/mBio.00480-13. PubMed PMID: 23882017; PubMed Central PMCID:
882 PMCPMC3735181.

883 82. Cascales E, Buchanan SK, Duche D, Kleanthous C, Lloubes R, Postle K, et al. Colicin
884 biology. *Microbiol Mol Biol Rev*. 2007;71(1):158-229. Epub 2007/03/10. doi:

- 885 10.1128/MMBR.00036-06. PubMed PMID: 17347522; PubMed Central PMCID:
886 PMCPMC1847374.
- 887 83. Ruhe ZC, Low DA, Hayes CS. Polymorphic toxins and their immunity proteins: diversity,
888 evolution, and mechanisms of delivery. *Annu Rev Microbiol.* 2020. Epub 2020/07/19. doi:
889 10.1146/annurev-micro-020518-115638. PubMed PMID: 32680451.
- 890 84. Kohler T, Donner V, van Delden C. Lipopolysaccharide as shield and receptor for R-
891 pyocin-mediated killing in *Pseudomonas aeruginosa*. *J Bacteriol.* 2010;192(7):1921-8. Epub
892 2010/02/02. doi: 10.1128/JB.01459-09. PubMed PMID: 20118263; PubMed Central PMCID:
893 PMCPMC2838038.
- 894 85. Ruhe ZC, Nguyen JY, Xiong J, Koskiniemi S, Beck CM, Perkins BR, et al. CdiA effectors
895 use modular receptor-binding domains to recognize target bacteria. *mBio.* 2017;8(2). Epub
896 2017/03/30. doi: 10.1128/mBio.00290-17. PubMed PMID: 28351921; PubMed Central PMCID:
897 PMCPMC5371414.
- 898 86. Willett JL, Gucinski GC, Fatherree JP, Low DA, Hayes CS. Contact-dependent growth
899 inhibition toxins exploit multiple independent cell-entry pathways. *Proc Natl Acad Sci U S A.*
900 2015;112(36):11341-6. Epub 2015/08/26. doi: 10.1073/pnas.1512124112. PubMed PMID:
901 26305955; PubMed Central PMCID: PMCPMC4568652.
- 902 87. Coulthurst S. The type VI secretion system: a versatile bacterial weapon. *Microbiology.*
903 2019;165(5):503-15. Epub 2019/03/21. doi: 10.1099/mic.0.000789. PubMed PMID: 30893029.
- 904 88. Krasauskas R, Skerniškytė J, Martinkus J, Armalytė J, Sužiedėlienė E. Capsule protects
905 *Acinetobacter baumannii* from inter-bacterial competition mediated by CdiA toxin. *Frontiers in*
906 *Microbiology.* 2020;11(1493). doi: 10.3389/fmicb.2020.01493.

- 907 89. Aoki SK, Malinverni JC, Jacoby K, Thomas B, Pamma R, Trinh BN, et al. Contact-
908 dependent growth inhibition requires the essential outer membrane protein BamA (YaeT) as the
909 receptor and the inner membrane transport protein AcrB. *Mol Microbiol.* 2008;70(2):323-40.
910 Epub 2008/09/03. doi: 10.1111/j.1365-2958.2008.06404.x. PubMed PMID: 18761695; PubMed
911 Central PMCID: PMCPMC2579741.
- 912 90. Virtanen P, Wäneskog M, Koskiniemi S. Class II contact-dependent growth inhibition
913 (CDI) systems allow for broad-range cross-species toxin delivery within the Enterobacteriaceae
914 family. *Mol Microbiol.* 2019;111(4):1109-25. Epub 2019/03/18. doi: 10.1111/mmi.14214.
915 PubMed PMID: 30710431; PubMed Central PMCID: PMCPMC6850196.
- 916 91. Flores-Mireles AL, Walker JN, Caparon M, Hultgren SJ. Urinary tract infections:
917 epidemiology, mechanisms of infection and treatment options. *Nat Rev Microbiol.*
918 2015;13(5):269-84. Epub 2015/04/09. doi: 10.1038/nrmicro3432. PubMed PMID: 25853778;
919 PubMed Central PMCID: PMCPMC4457377.
- 920 92. Giacometti A, Cirioni O, Schimizzi AM, Del Prete MS, Barchiesi F, D'Errico MM, et al.
921 Epidemiology and microbiology of surgical wound infections. *J Clin Microbiol.* 2000;38(2):918-
922 22. Epub 2000/02/03. PubMed PMID: 10655417; PubMed Central PMCID: PMCPMC86247.
- 923 93. Keogh D, Tay WH, Ho YY, Dale JL, Chen S, Umashankar S, et al. Enterococcal
924 metabolite cues facilitate interspecies niche modulation and polymicrobial infection. *Cell Host*
925 *Microbe.* 2016;20(4):493-503. Epub 2016/10/14. doi: 10.1016/j.chom.2016.09.004. PubMed
926 PMID: 27736645; PubMed Central PMCID: PMCPMC5076562.
- 927 94. Goh HMS, Yong MHA, Chong KKL, Kline KA. Model systems for the study of
928 enterococcal colonization and infection. *Virulence.* 2017;8(8):1525-62. Epub 2017/01/20. doi:

- 929 10.1080/21505594.2017.1279766. PubMed PMID: 28102784; PubMed Central PMCID:
930 PMCPMC5810481.
- 931 95. King KC, Brockhurst MA, Vasieva O, Paterson S, Betts A, Ford SA, et al. Rapid
932 evolution of microbe-mediated protection against pathogens in a worm host. *ISME J.*
933 2016;10(8):1915-24. Epub 2016/03/16. doi: 10.1038/ismej.2015.259. PubMed PMID: 26978164;
934 PubMed Central PMCID: PMCPMC5029159.
- 935 96. Hammer ND, Cassat JE, Noto MJ, Lojek LJ, Chadha AD, Schmitz JE, et al. Inter- and
936 intraspecies metabolite exchange promotes virulence of antibiotic-resistant *Staphylococcus*
937 *aureus*. *Cell Host Microbe.* 2014;16(4):531-7. Epub 2014/10/10. doi:
938 10.1016/j.chom.2014.09.002. PubMed PMID: 25299336; PubMed Central PMCID:
939 PMCPMC4197139.
- 940 97. Sullivan MJ, Petty NK, Beatson SA. Easyfig: a genome comparison visualizer.
941 *Bioinformatics.* 2011;27(7):1009-10. Epub 2011/01/28. doi: 10.1093/bioinformatics/btr039.
942 PubMed PMID: 21278367; PubMed Central PMCID: PMCPMC3065679.
- 943 98. Kanehisa M, Goto S. KEGG: kyoto encyclopedia of genes and genomes. *Nucleic Acids*
944 *Res.* 2000;28(1):27-30. doi: 10.1093/nar/28.1.27. PubMed PMID: 10592173; PubMed Central
945 PMCID: PMCPMC102409.
- 946 99. Sigrist CJ, de Castro E, Cerutti L, Cucho BA, Hulo N, Bridge A, et al. New and
947 continuing developments at PROSITE. *Nucleic Acids Res.* 2013;41(Database issue):D344-7.
948 Epub 2012/11/17. doi: 10.1093/nar/gks1067. PubMed PMID: 23161676; PubMed Central
949 PMCID: PMCPMC3531220.
- 950 100. DeLano WD. The PyMOL Molecular Graphics System, 1.3. Schroedinger, LLC2010.

- 951 101. Kumar S, Stecher G, Li M, Knyaz C, Tamura K. MEGA X: Molecular Evolutionary
952 Genetics Analysis across computing platforms. *Mol Biol Evol.* 2018;35(6):1547-9. doi:
953 10.1093/molbev/msy096. PubMed PMID: 29722887; PubMed Central PMCID:
954 PMCPMC5967553.
- 955 102. Coordinators NR. Database resources of the National Center for Biotechnology
956 Information. *Nucleic Acids Res.* 2018;46(D1):D8-D13. doi: 10.1093/nar/gkx1095. PubMed
957 PMID: 29140470; PubMed Central PMCID: PMCPMC5753372.
- 958 103. Letunic I, Bork P. Interactive Tree Of Life (iTOL) v4: recent updates and new
959 developments. *Nucleic Acids Res.* 2019;47(W1):W256-W9. doi: 10.1093/nar/gkz239. PubMed
960 PMID: 30931475; PubMed Central PMCID: PMCPMC6602468.
- 961 104. Geer LY, Domrachev M, Lipman DJ, Bryant SH. CDART: protein homology by domain
962 architecture. *Genome Res.* 2002;12(10):1619-23. doi: 10.1101/gr.278202. PubMed PMID:
963 12368255; PubMed Central PMCID: PMCPMC187533.
- 964 105. Barnes WM. PCR amplification of up to 35-kb DNA with high fidelity and high yield from
965 lambda bacteriophage templates. *Proc Natl Acad Sci U S A.* 1994;91(6):2216-20. Epub
966 1994/03/15. PubMed PMID: 8134376; PubMed Central PMCID: PMCPMC43341.
- 967 106. Gibson DG, Young L, Chuang RY, Venter JC, Hutchison CA, 3rd, Smith HO. Enzymatic
968 assembly of DNA molecules up to several hundred kilobases. *Nat Methods.* 2009;6(5):343-5.
969 Epub 2009/04/14. doi: 10.1038/nmeth.1318. PubMed PMID: 19363495.
- 970 107. Thurlow LR, Thomas VC, Hancock LE. Capsular polysaccharide production in
971 *Enterococcus faecalis* and contribution of CpsF to capsule serospecificity. *J Bacteriol.*
972 2009;191(20):6203-10. Epub 2009/08/18. doi: 10.1128/JB.00592-09. PubMed PMID: 19684130;
973 PubMed Central PMCID: PMCPMC2753019.

974 108. Krogh A, Larsson B, von Heijne G, Sonnhammer EL. Predicting transmembrane protein
975 topology with a hidden Markov model: application to complete genomes. J Mol Biol.
976 2001;305(3):567-80. doi: 10.1006/jmbi.2000.4315. PubMed PMID: 11152613.

977

978 **Acknowledgments**

979 This work was supported by National Institutes of Health grants R01AI141479 (B.A.D.) and
980 R01AI122742 (G.M.D.). J.L.E.W. was supported by American Heart Association Grant
981 19POST34450124 / Julia Willett / 2018. We would like to thank Andrés Vázquez-Torres, Laurel
982 Lenz, Alex Horswill, Stefan Pukatzki, Kelly Doran, and their lab members for sharing bacterial
983 strains used in this study. We thank Michelle Korir for the *ireK* complementation plasmid
984 construct and strain.

985

986 **Author Contributions**

987 A.C., J.L.E.W., G.M.D. and B.A.D. designed the study. A.C. and J.L.E.W. performed
988 experiments and bioinformatic analyses. A.C., J.L.E.W., G.M.D. and B.A.D. analyzed data. A.C.,
989 J.L.E.W. and B.A.D. wrote the paper with input from G.M.D.

990

991 **Corresponding author**

992 Address correspondence to Breck A. Duerkop breck.duerkop@cuanschutz.edu

993

994 **Competing Interests**

995 There are no competing interests to report for this work.

996

997 **Figure Legends**

998

999 **Figure 1. Phage mediated inhibition of bystander bacteria is dependent on enterococcal**
1000 **T7SS. (A)** Diagram showing the location of T7SS genes in *E. faecalis* OG1RF (NC_017316.1)
1001 compared to *E. faecalis* V583 (NC_004668.1). Sequences were obtained from NCBI, and
1002 homology comparisons were rendered in EasyFig. Nucleotide alignments generated by Clustal
1003 Omega are enlarged for clarity (dashed lines). Stop codons of genes EF1328/OG1RF_11099
1004 and EF1337/OG1RF_11127 are boxed. **(B)** Schematic representation of the co-culture assay
1005 used to assess the viability of bystander bacteria during phage induced T7SS activity of wild
1006 type *E. faecalis* OG1RF and Δ essB. Relative viability of bystander strains is calculated by
1007 measuring the ratio of bystander cfus in the phage infected culture compared to the bystander
1008 cfus from an uninfected control culture. **(C)** The relative abundance of viable bystander
1009 bacterium *E. faecalis* Δ pip_{V583}. Complementation of the *E. faecalis* Δ essB mutant, Δ essB
1010 (pLZ12A::essB), restores T7SS dependent bystander inhibition. Δ essB (pLZ12A) is the empty
1011 vector control. **(D)** T7SS inhibition of other bacterial species in the presence and absence of
1012 phage infected *E. faecalis* OG1RF or Δ essB. Data represent three biological replicates. Error
1013 bars indicate standard deviation. * $P < 0.00001$ by unpaired Student's t-test.

1014

1015 **Figure 2. Identification of *E. faecalis* T7SS toxin and immunity proteins that dictate**
1016 **bystander growth inhibition. (A)** Putative toxin-encoding genes in the OG1RF T7SS locus.
1017 LXG domains in OG1RF_11109 and OG1RF_11121 were identified using KEGG and ExPASy
1018 PROSITE. Putative orphan toxins were identified by homology to OG1RF_11109 or
1019 OG1RF_11121. Gray lines between diagrams indicate the regions and degree of nucleotide
1020 conservation between genes. Homology diagrams were rendered in EasyFig. Gene colors for
1021 OG1RF_11109, OG1RF_11111, and OG1RF_11121 match the color scheme in panel **(B)**.
1022 OG1RF_11113 and OG1RF_11123 are shaded black to indicate that their corresponding
1023 immunity genes were not tested in panel **(B)**. **(B)** *E. faecalis* OG1RF T7SS mediated growth
1024 inhibition of phage resistant *E. faecalis* Δ pip_{V583} during infection is alleviated by expressing

1025 OG1RF_11122 in *E. faecalis* Δpip_{V583} but not in the presence of pLZ12A empty vector, or
1026 expressing OG1RF_11110, OG1RF_11112, or OG1RF_12413. **(C – D)** Disruption of
1027 OG1RF_11121 by a transposon insertion rescues growth of phage resistant *E. faecalis* Δpip_{V583}
1028 **(C)** and *S. aureus* **(D)** strains during co-culture. Complementation of OG1RF_11121-Tn restores
1029 bystander intoxication. Data represent three biological replicates. Error bars indicate standard
1030 deviation. * $P < 0.0001$ by unpaired Student's t-test.

1031
1032 **Figure 3. Sub-lethal antibiotic treatment enhances T7SS gene expression leading to**
1033 **inhibition of bystander bacteria.** Altered expression of T7SS genes upon exposure to sub-
1034 inhibitory concentrations of **(A)** ampicillin (0.19 $\mu\text{g/ml}$), vancomycin (0.78 $\mu\text{g/ml}$) or daptomycin
1035 (6.25 $\mu\text{g/ml}$) and **(B)** ciprofloxacin (2 $\mu\text{g/ml}$) or mitomycin C (4 $\mu\text{g/ml}$) for 40 minutes relative to
1036 the untreated control. *clpX* is shown as a negative control. **(C-E)** Contact-dependent T7SS
1037 mediated inhibition of bystander bacteria in the presence of daptomycin. Relative viability of *E.*
1038 *faecalis* Δpip_{V583} was measured during co-culture with *E. faecalis* OG1RF or $\Delta essB$ antagonists
1039 in the presence and absence of daptomycin treatment in **(C)** liquid culture (2.5 $\mu\text{g/ml}$
1040 daptomycin), **(D)** trans-well plates to prevent physical engagement between cells (2.5 $\mu\text{g/ml}$
1041 daptomycin) and **(E)** in contact on agar media (0.5 $\mu\text{g/ml}$ daptomycin). $\Delta essB$ (pLZ12A) and
1042 $\Delta essB$ (pLZ12A::*essB*) represent the empty vector control and complemented strains. Data
1043 show three biological replicates. Error bars indicate standard deviation. * $P < 0.01$, ** $P < 0.001$ to
1044 0.0001 by unpaired Student's t-test.

1045
1046 **Figure 4. IreK and OG1RF_11099 control transcription of enterococcal T7SS genes and**
1047 **subsequent inhibition of bystander bacteria during phage infection.** **(A)** Phage infection
1048 leads to enhanced expression of T7SS genes in wild type *E. faecalis* OG1RF but not in a $\Delta ireK$
1049 mutant strain. **(B)** Growth inhibition of *E. faecalis* Δpip_{V583} during phage infection of *E. faecalis*
1050 OG1RF is abrogated in the $\Delta essB$ and $\Delta ireK$ mutants carrying empty pCIEtm. pCIEtm::*ireK*

1051 complemented the T7SS activity defect of the $\Delta ireK$ strain. **(C)** Disruption of OG1RF_11099
1052 leads to reduced expression of T7SS genes during phage infection. The data are represented
1053 as the fold change of normalized mRNA relative to uninfected samples at the same time
1054 points. **(D)** T7SS dependent intraspecies antagonism during phage infection is alleviated in the
1055 presence of OG1RF_11099-Tn mutant carrying empty pCIEtm. pCIEtm::11099 complemented
1056 the T7SS activity defect of the OG1RF_11099-Tn mutant strain. Data represent three biological
1057 replicates. Error bars indicate standard deviation. $*P < 0.00001$ by unpaired Student's t-test.

1058

1059 **Figure 5. A model for inhibition of bystander bacteria by the *E. faecalis* OG1RF T7SS.**

1060 Phage and select antibiotics trigger a response involving IreK that results in induction of
1061 expression of T7SS genes. Transcription of T7SS genes is regulated by the predicted GntR-
1062 family transcription factor OG1RF_11099. The predicted core components of the OG1RF T7SS
1063 machinery are putative membrane proteins EsaA (OG1RF_11101), OG1RF_11102, EssB
1064 (OG1RF_11104), and EssC1 (OG1RF_11105) as well as the putative cytoplasmic protein EsaB
1065 (OG1RF_11103). EssC2 (OG1RF_11115) lacks transmembrane domains and is thus not
1066 predicted to be membrane-anchored. Upon induction of the T7SS, OG1RF_11121 is secreted
1067 from the cell, resulting in antibacterial activity against select neighboring bacteria. Expression of
1068 OG1RF_11122 can partially block toxicity caused by OG1RF_11121. Predictions of membrane
1069 topology were obtained using TMHMM [108]. The figure was created with Biorender.com.

1070

1071 **Figure S1. Phylogenetic tree of EsxA sequences in *enterococci*.** Non-redundant sequences
1072 (n=96) were identified using NCBI BLAST with OG1RF EsxA (OG1RF_11100) as the input. The
1073 tree was constructed in MEGAX using the Maximum Likelihood method and JTT matrix-based
1074 model and is drawn to scale, with branch lengths measured in the number of substitutions per
1075 site. The tree with the highest log likelihood (-3544.39) is shown. *E. faecalis* sequences are

1076 highlighted in purple, and the GenBank identifier for EsxA from OG1RF (AEA93787.1) is shown
1077 in red font.

1078

1079 **Figure S2. Phage VPE25 infects wild type *E. faecalis* OG1RF and T7SS mutants with**
1080 **similar efficacy. (A)** The measurement of phage particles released from wild type *E. faecalis*
1081 OG1RF, Δ essB, OG1RF_11121-Tn, and OG1RF_11099-Tn mutant strains following phage
1082 VPE25 infection. **(B)** Viability of strains of the OG1RF background exhibiting differential T7SS
1083 activity in the absence and presence of phage. **(C)** Viability of T7SS susceptible strains during
1084 intraspecies competition experiments in the absence and presence of phage. Data represent
1085 three biological replicates. Error bars indicate standard deviation. * $P < 0.0001$ by unpaired
1086 Student's t-test.

1087

1088 **Figure S3. Phage induced T7SS inhibitory activity is contact dependent.** Intraspecies
1089 competition experiment performed in the presence of unfiltered supernatant from phage treated
1090 and untreated *E. faecalis* wild type OG1RF or Δ essB added **(A)** to the top of a well separated by
1091 a 0.4 μ m membrane from the bottom well containing *E. faecalis* Δ pip_{V583} culture, and bacterial
1092 viability was determined after 24 hours, or **(B)** directly into *E. faecalis* Δ pip_{V583} culture in
1093 microtiter plate wells ($P = 0.7955$ by two-way analysis of variance [ANOVA]). **(C)** Growth of
1094 Δ pip_{V583} was monitored in the presence of filtered supernatant from uninfected and phage
1095 infected cultures of wild type *E. faecalis* OG1RF and Δ essB ($P = 0.0883$ by two-way analysis of
1096 variance [ANOVA]). *E. faecalis* Δ pip_{V583} cultures in all of these three contact-dependent assays
1097 contained gentamicin (25 μ g/ml) to prevent growth of the OG1RF background strains that may
1098 have carried over in unfiltered supernatants. Error bars indicate standard deviation.

1099

1100 **Figure S4. Putative orphan toxins in OG1RF are found as full-length LXG-domain**
1101 **proteins in other bacteria.** OG1RF_11111, OG1RF_11113, and OG1RF_11123 sequences
1102 were used as input for NCBI BLAST. Alignments and homology were rendered in EasyFig.

1103

1104 **Figure S5. A distal *E. faecalis* OG1RF locus encodes an additional LXG-domain protein.**

1105 **(A)** Schematic showing homology between V583 (NC_004668.1, top) and OG1RF
1106 (NC_017316.1, bottom). Sequences were obtained from NCBI, and homology comparisons
1107 were rendered in EasyFig. **(B)** Cartoon depicting the LXG domain of OG1RF_12414 (identified
1108 using KEGG and ExpASY PROSITE). **(C)** Predicted structural homology between
1109 OG1RF_12414 (lilac) and the *Pseudomonas protogens* Pf-5 Tne2/Tni2 complex (PDB 6B12).
1110 Tne2 is shown in green, and Tni2 is shown in gray. Structural modeling was done using
1111 PHYRE2, and images were rendered in Pymol.

1112

1113 **Figure S6. Domain architecture of enterococcal LXG proteins.** Domain architectures were
1114 identified using the NCBI Conserved Domain Architectural Retrieval Tool (DART) with
1115 OG1RF_11109 as an input. Diagrams are drawn to scale.

1116

1117 **Figure S7. Antibiotic susceptibility of *E. faecalis* OG1RF.** Growth of wild type *E. faecalis*
1118 OG1RF was monitored over 20 hours in the presence or absence of **(A)** ampicillin, **(B)**
1119 vancomycin and **(C)** daptomycin in microtiter plates. The antibiotic concentrations highlighted
1120 with a blue box were deemed sub-inhibitory and used to investigate T7SS gene expression
1121 levels. Early log-phase cultures of *E. faecalis* OG1RF were grown in the presence or absence of
1122 **(D)** mitomycin C (4 µg/ml) or **(E)** ciprofloxacin (2 µg/ml) to show that these concentrations of
1123 DNA targeting antibiotics do not prevent bacterial growth. Error bars indicate standard deviation.

1124

1125 **Figure S8. Impact of daptomycin concentration on *E. faecalis* growth and T7SS induction.**

1126 Growth of different enterococcal strains either untreated or treated with 6.25 µg/ml, 2.5 µg/ml or
1127 0.5 µg/ml of daptomycin in **(A – C)** liquid media. **(D)** T7SS transcripts were measured from *E.*
1128 *faecalis* OG1RF cells grown in liquid media containing either no daptomycin or 6.25 µg/ml, 2.5
1129 µg/ml, or 0.5 µg/ml of daptomycin. The data are expressed as the average of three biological
1130 replicates ± the standard deviation. $P < 0.001$ by unpaired Student's t-test. **(E)** Viable bacterial
1131 cells recovered from growth on daptomycin supplemented agar media for 24 hours. The dashed
1132 line indicates the limit of detection.

1133

1134 **Figure S9. Effect of sub-lethal bile salt treatment on growth and T7SS transcription in *E.***

1135 ***faecalis* OG1RF.** **(A)** Optical density of wild type *E. faecalis* OG1RF grown in the absence and
1136 presence of 4% sodium cholate was measured for 18 hours. **(B)** Transcript levels of OG1RF
1137 T7SS genes in untreated and 4% sodium cholate treated *E. faecalis* OG1RF after 4 hours. $P <$
1138 0.001 to by unpaired Student's t-test. Error bars indicate standard deviation.

1139

1140 **Figure S10. *E. faecalis* mutants of cell wall homeostasis show no growth defects and**

1141 **respond to phage VPE25 infection.** **(A)** Optical density of wild type *E. faecalis* OG1RF and
1142 isogenic mutants were monitored for 18 hours. **(B)** While all strains were susceptible to phage
1143 VPE25 infection, the proportion of released phage particles was diminished in the *croR* and
1144 *croS* transposon mutant background. Data represent three biological replicates. Error bars
1145 indicate standard deviation. $*P < 0.001$ by unpaired Student's t-test.

1146

1147 **Figure S11. Quantitative PCR demonstrates that LiaR/S and CroS/R two-component**
1148 **systems do not influence T7SS gene expression during phage infection.** **(A- F)** mRNA

1149 transcript levels of T7SS genes are enhanced in the transposon mutants of *liaR*, *liaS*, *croR* and
1150 *croS* strains similar to wild type *E. faecalis* OG1RF during phage infection (MOI = 1) compared

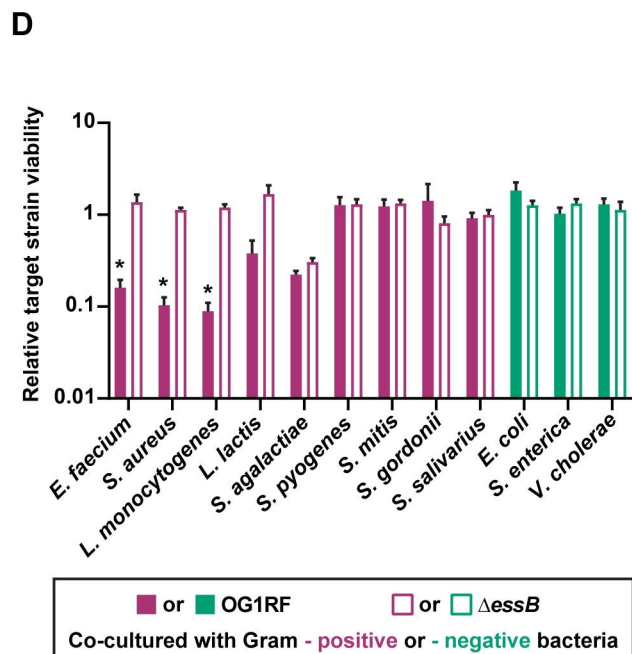
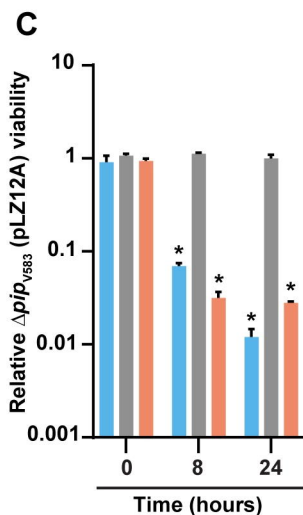
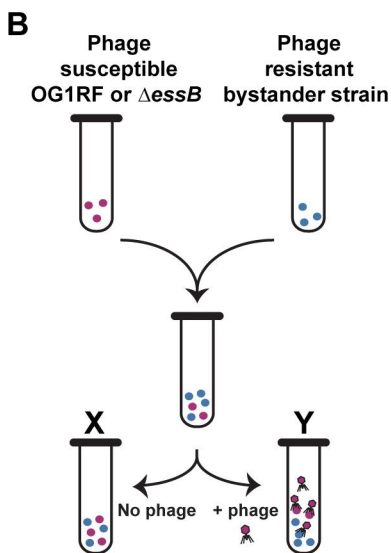
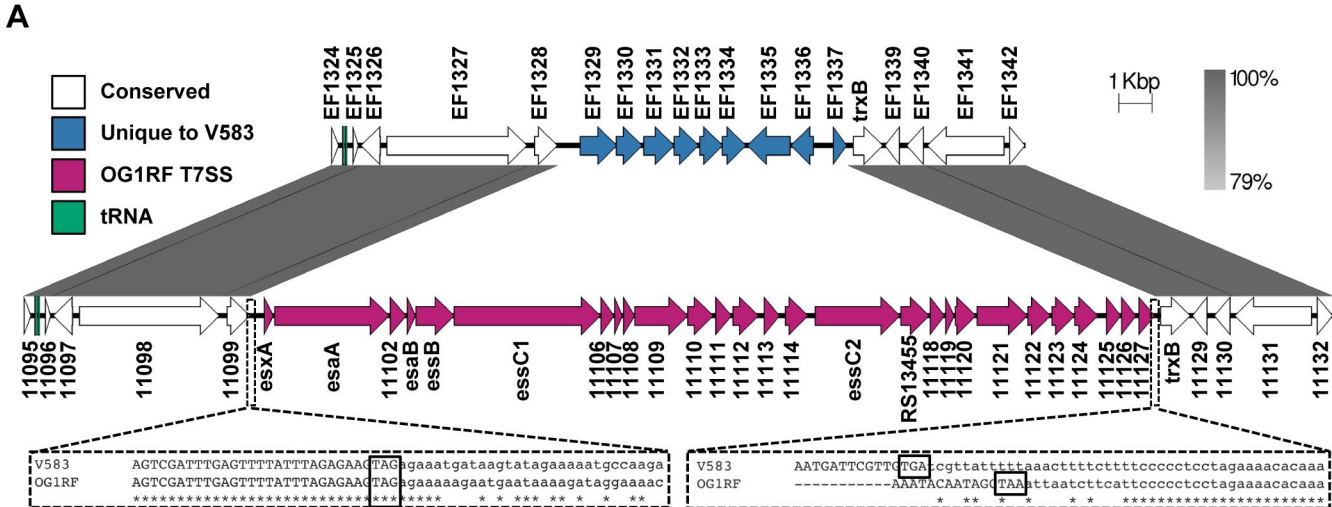
1151 to untreated controls. Data represent three biological replicates. Error bars indicate standard
1152 deviation. * $P < 0.01$, ** $P < 0.0001$ by unpaired Student's t-test.

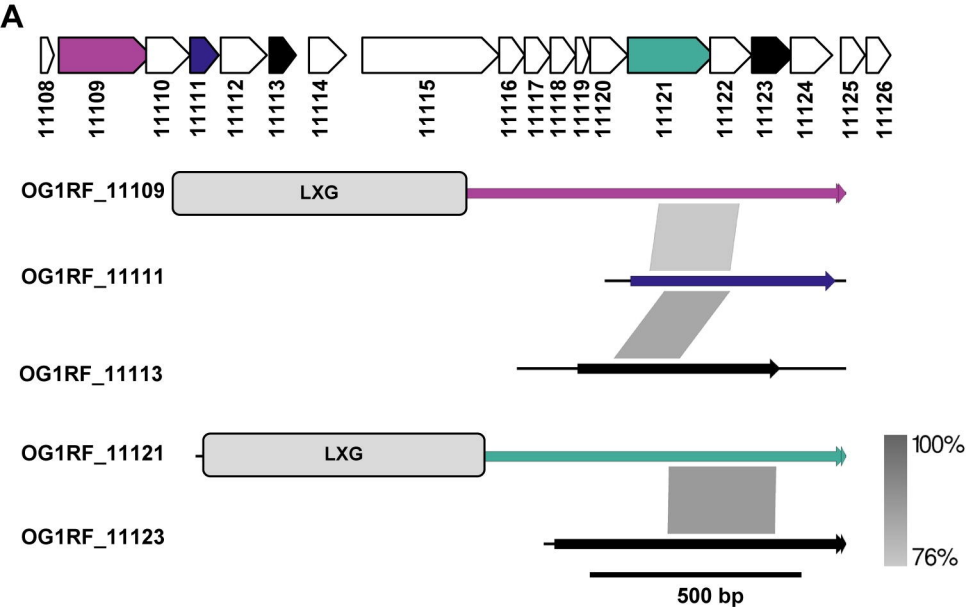
1153

1154 **Figure S12. Influence of sub-lethal ceftriaxone challenge and phage infection on the**
1155 **expression of *E. faecalis* T7SS genes. (A)** Transcription of T7SS genes in *E. faecalis* OG1RF
1156 are not elevated 20 minutes post ceftriaxone (128 μ g/ml) administration relative to an untreated
1157 control. **(B)** OG1RF_11099 expression remains unaltered during phage predation of wild type *E.*
1158 *faecalis* OG1RF and $\Delta ireK$ strains relative to uninfected controls. Data represent three biological
1159 replicates. Error bars indicate standard deviation.

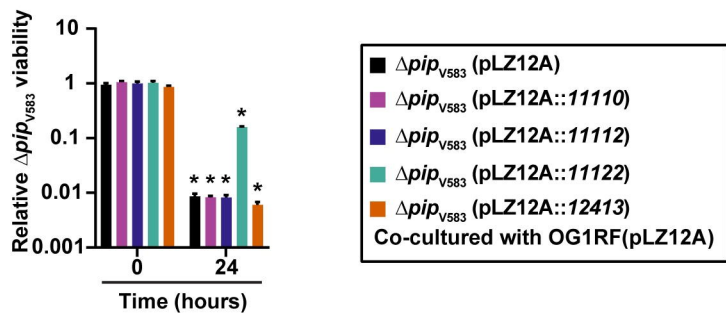
1160

1161 **Table S1. List of bacterial strains, phages, plasmids and primers used in this study.**

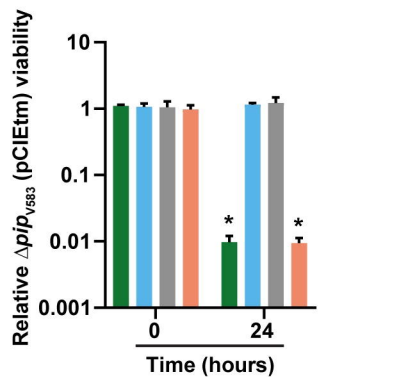




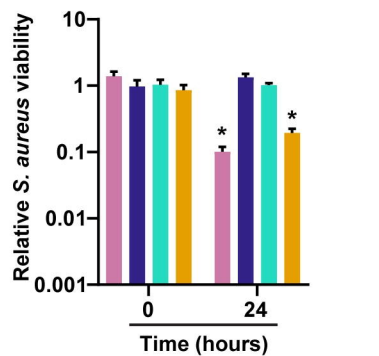
B

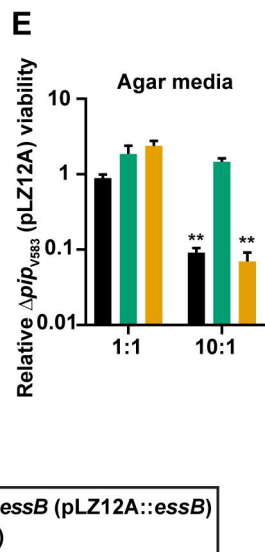
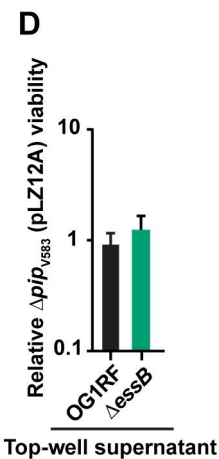
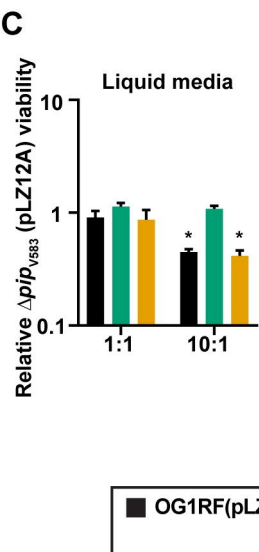
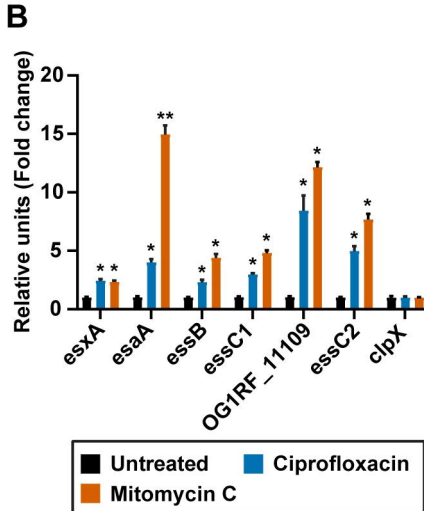
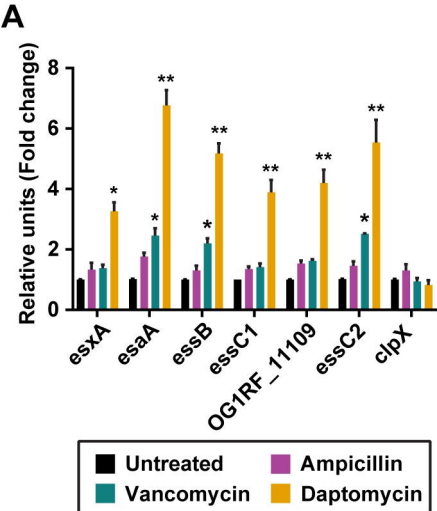


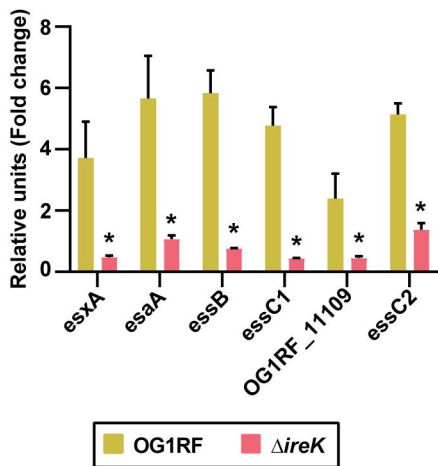
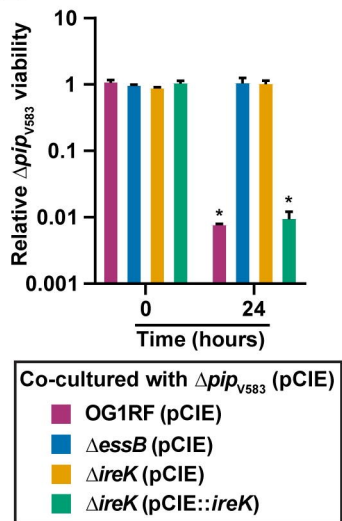
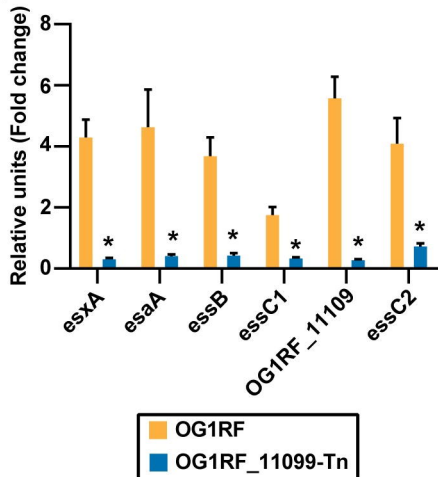
C



D





A**B****C****D**